X-ray Imaging

Wataru Yashiro
Graduate School of Frontier Sciences,
the University of Tokyo,
JAPAN

9th SESAME User meeting and KEK School
Amman, Jordan
12-16, November, 2011

OUTLINE

- Introduction – X-ray imaging
- Conventional X-ray absorption imaging & tomography
- X-ray phase imaging & tomography
  - Advantage of using X-ray phase information
  - Examples of X-ray phase imaging techniques
    - Interferometric method
    - Propagation-based method
    - Analyzer-based methods
- X-ray microscopy
  - Optics for X-ray microscopy
  - Examples of X-ray microscopies
    - X-ray imaging microscopy
    - Scanning transmission X-ray microscopy
    - X-ray diffraction microscopy (coherent diffractive imaging)
- Summary

X-ray imaging

Imaging

Mapping signal in space

↓

Mapping structure and /or property

↓

Used for Understanding function

Interaction of X-rays with matter

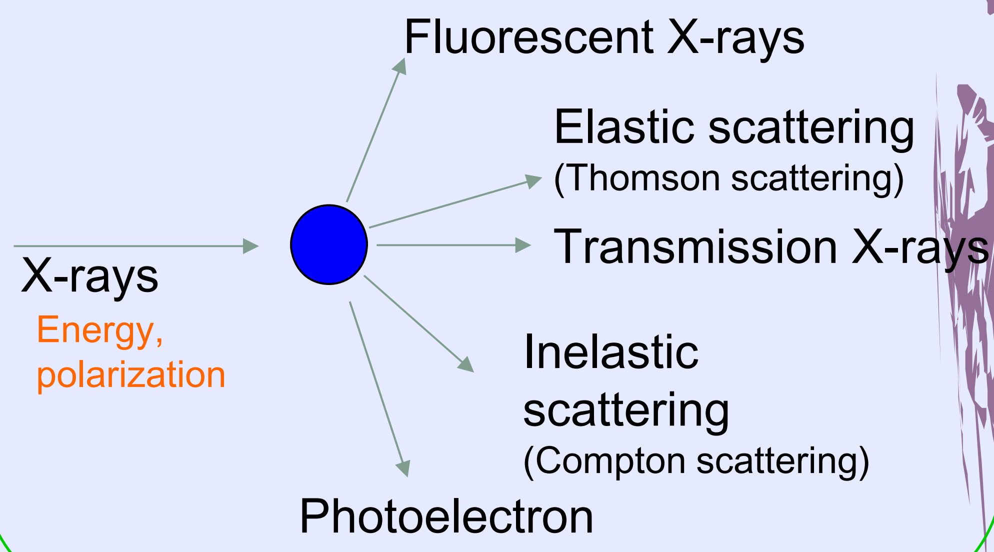

Ways for mapping

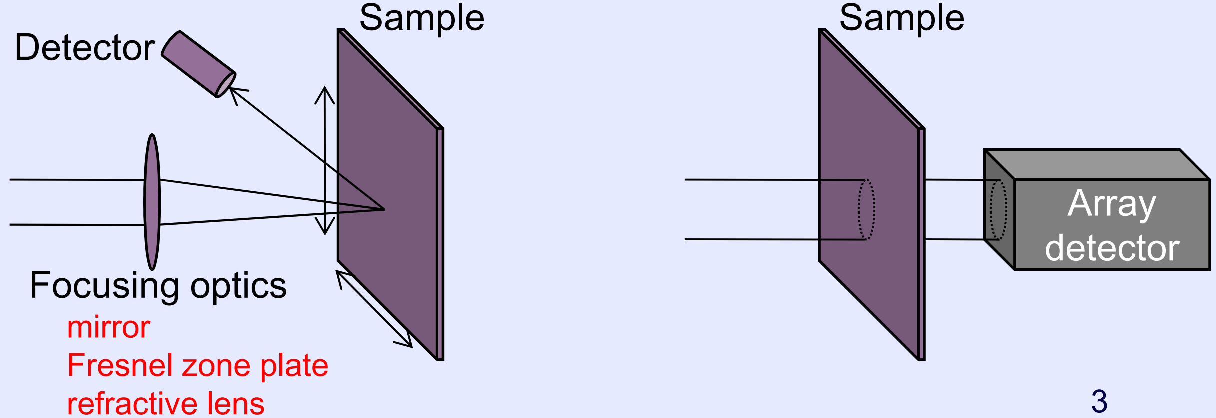

Applications

A wide range of science & technology, such as

- ➢Material science
- ➢Environmental science
- ➢Biology
- ➢Medicine
- ➢Archaeology
- ➢palaeontology
- ➢Industrial technology
- ➢…

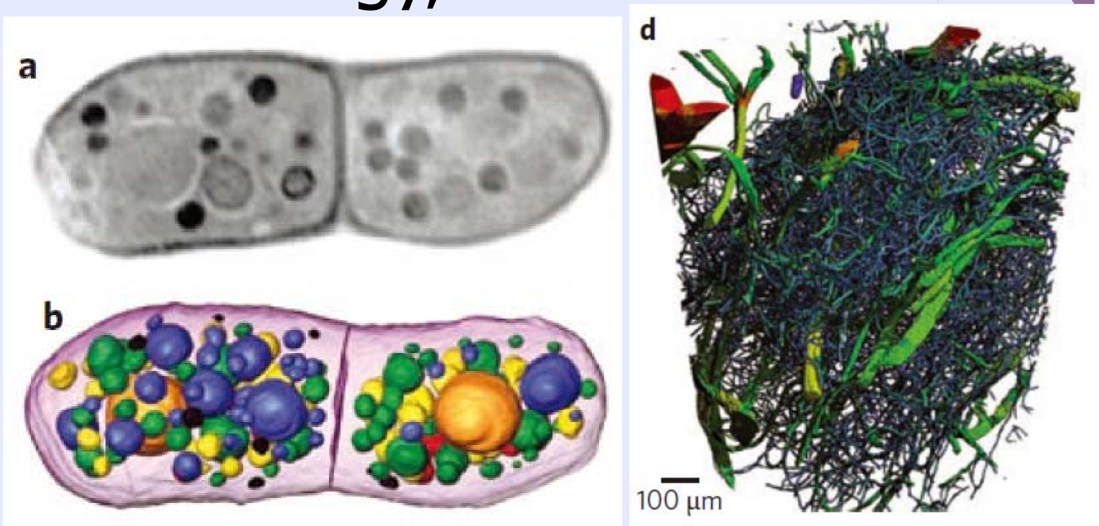

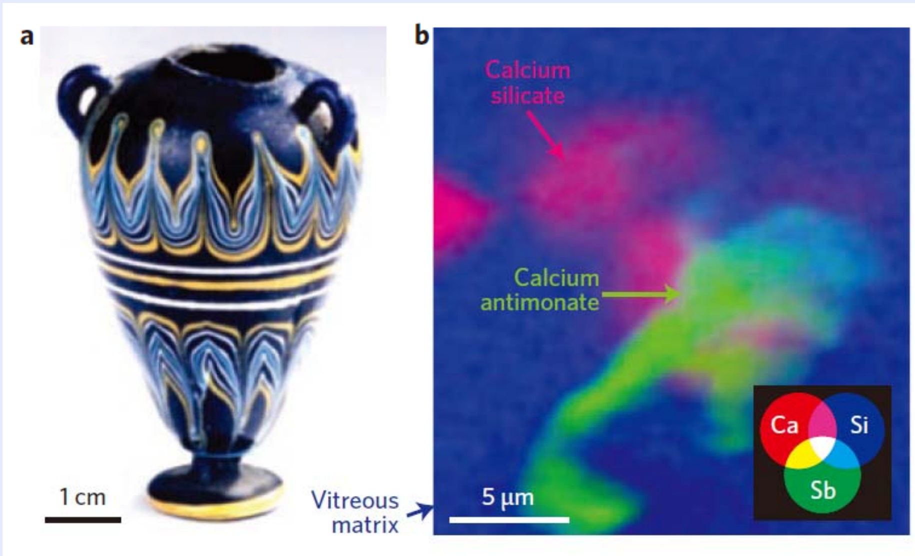

Anne Sakdinawat &David Attwood, *Nature Photonics* **4** (2010) 840.

X-ray transmission imaging

Discovery of X-rays （ Nov 1895　by Wilhelm Conrad Röntgen ）

Jan. 1896

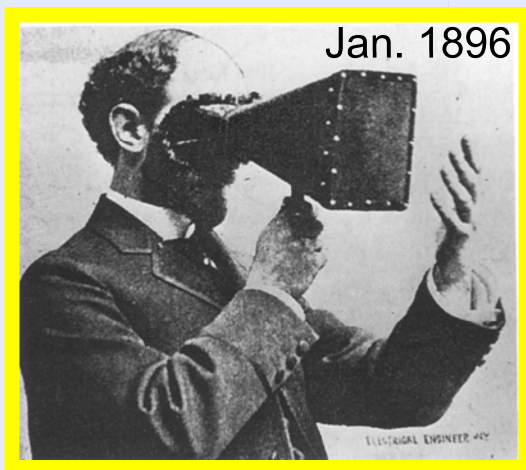

Jan. 1896

Fluoroscope

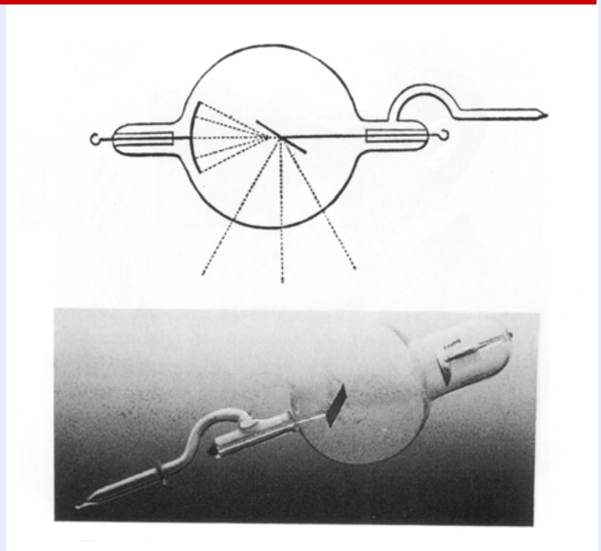

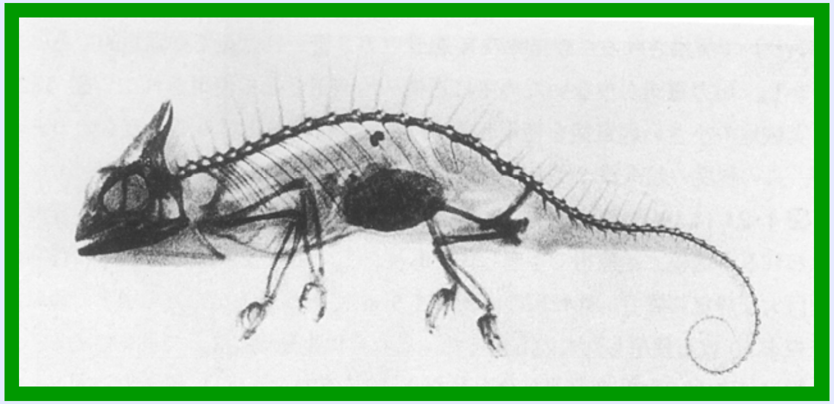

Computed Tomography (CT)

- A technique referring to imaging by sections or sectioning, through the use of any kind of penetrating wave.
- Invented by Godfrey Hounsfield & Allan Cormack.

X-ray CT

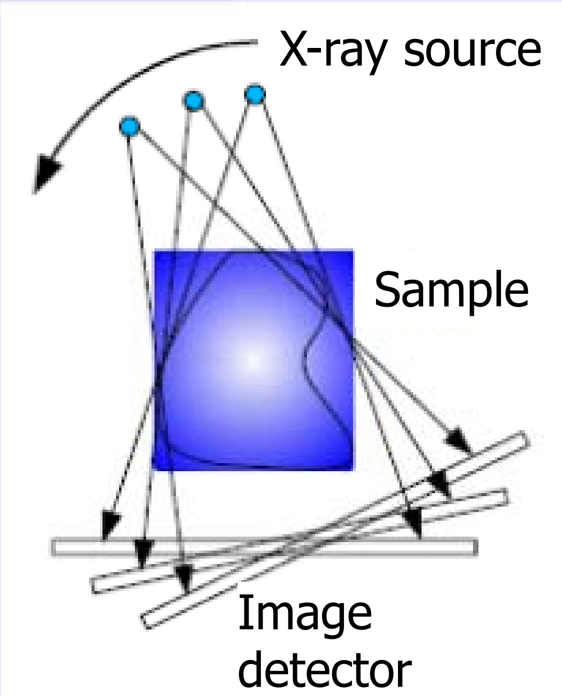

Capacitor

3D structure

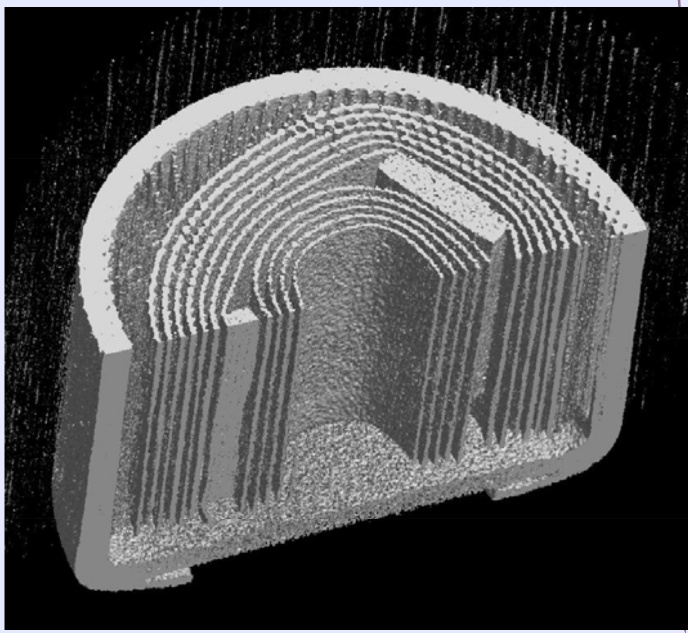

The sensitivity of conventional X-ray imaging is poor to soft matter and biological soft tissue

Airport X-ray scanner

Mail screening

Toward High-sensitive X-ray Imaging
— X-ray Phase Imaging

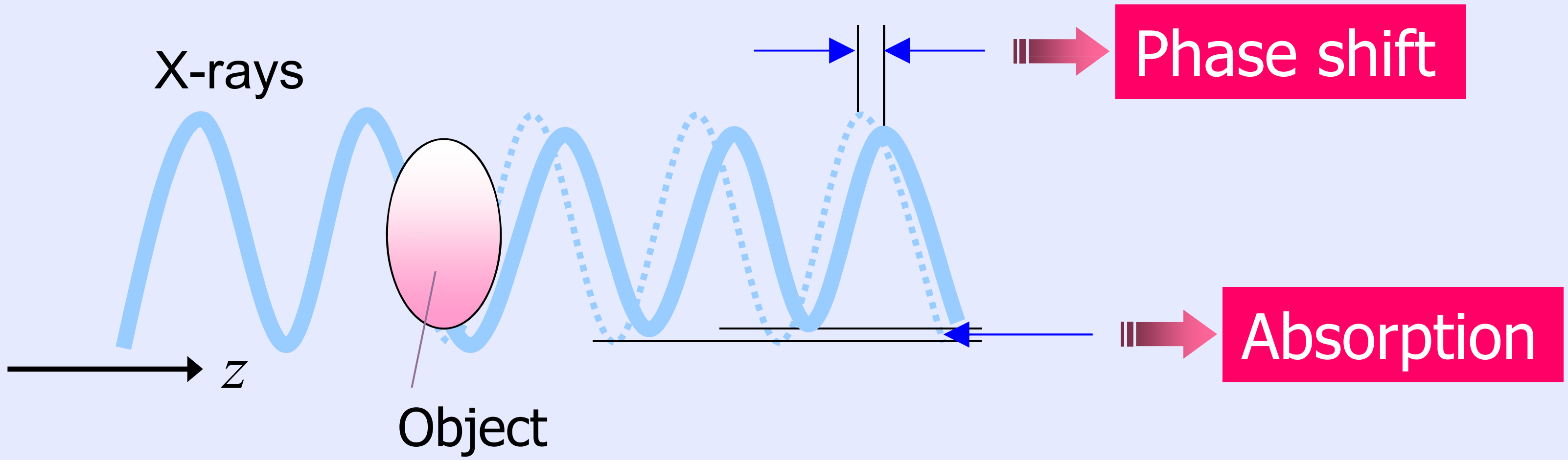

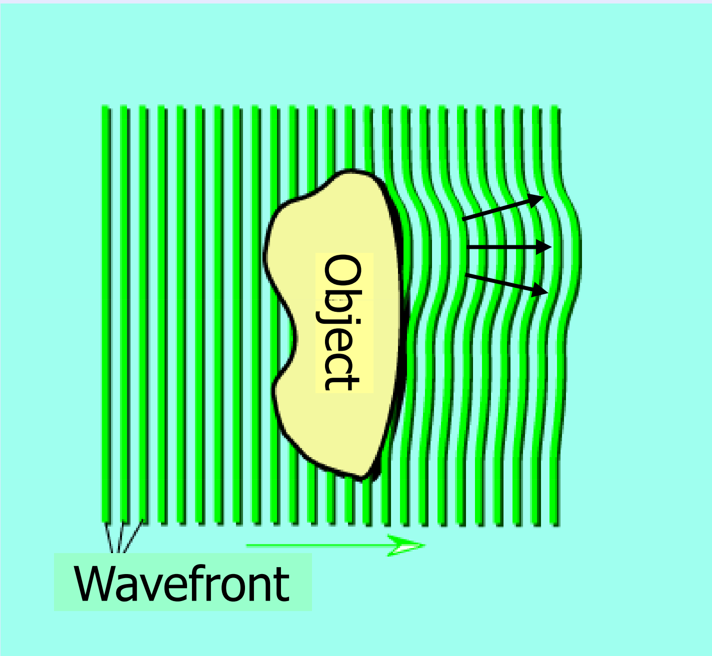

Refraction by the object (phase shift)
↓
Inclination of wavefront

Complex refractive index

X-rays
(Plane wave)

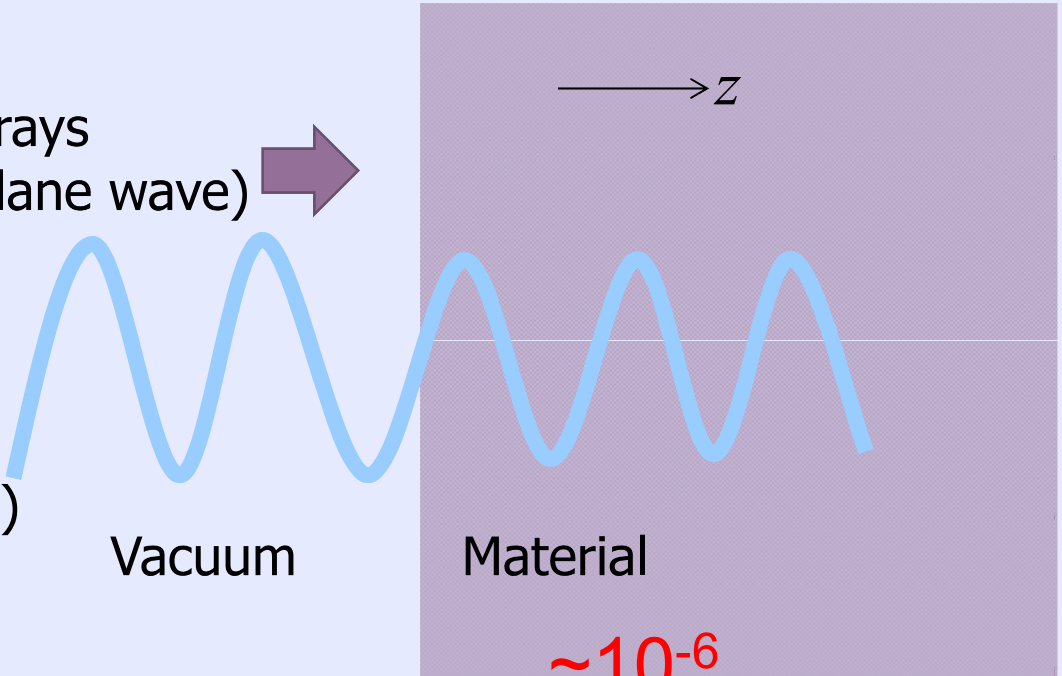

$$k \equiv \frac{2\pi}{\lambda}$$

(λ: wavelength)

~10^{-6}

	Vacuum	Material
Complex refractive index	$n = 1$	$n = 1 - \delta + i\beta$
Expression of plane wave	$\exp(ikz)$	$\exp(inkz) = \underbrace{\exp\left(2\pi i \frac{1-\delta}{\lambda} z\right)}_{\text{Phase shift}} \underbrace{\exp\left(-2\pi \frac{\beta}{\lambda} z\right)}_{\text{Absorption}}$

~10^{-9}

Phase shift: $\Delta = -2\pi \int \delta(x, y, z) dz / \lambda$

Relation between refractive index & atomic scattering factor

$$\delta = \frac{r_e \lambda^2}{2\pi} \sum_k N_k (Z_k + f'_k)$$

$$= \frac{\lambda}{2\pi} \sum_k N_k p_k \quad [p_k \equiv r_e \lambda (Z_k + f'_k)]$$

$$\beta = \frac{r_e \lambda^2}{2\pi} \sum_k N_k f''_k$$

$$= \frac{\lambda}{4\pi} \sum_k N_k \mu_k^a$$

N_k: atomic density
Z_k: atomic number
f'_k: read part of anomalous scattering factor
f''_k: imaginary part of anomalous scattering factor

λ: wavelength
r_e: classical electron radius

~10^{-6}

$$\boxed{1 - \delta + i\beta}$$

~10^{-9}

Atomic interaction cross sections of absorption ($\mu^a{}_k$) and phase shift (p_k) are responsible for the difference in image contrast.

Atomic number dependence of interaction cross section of atom

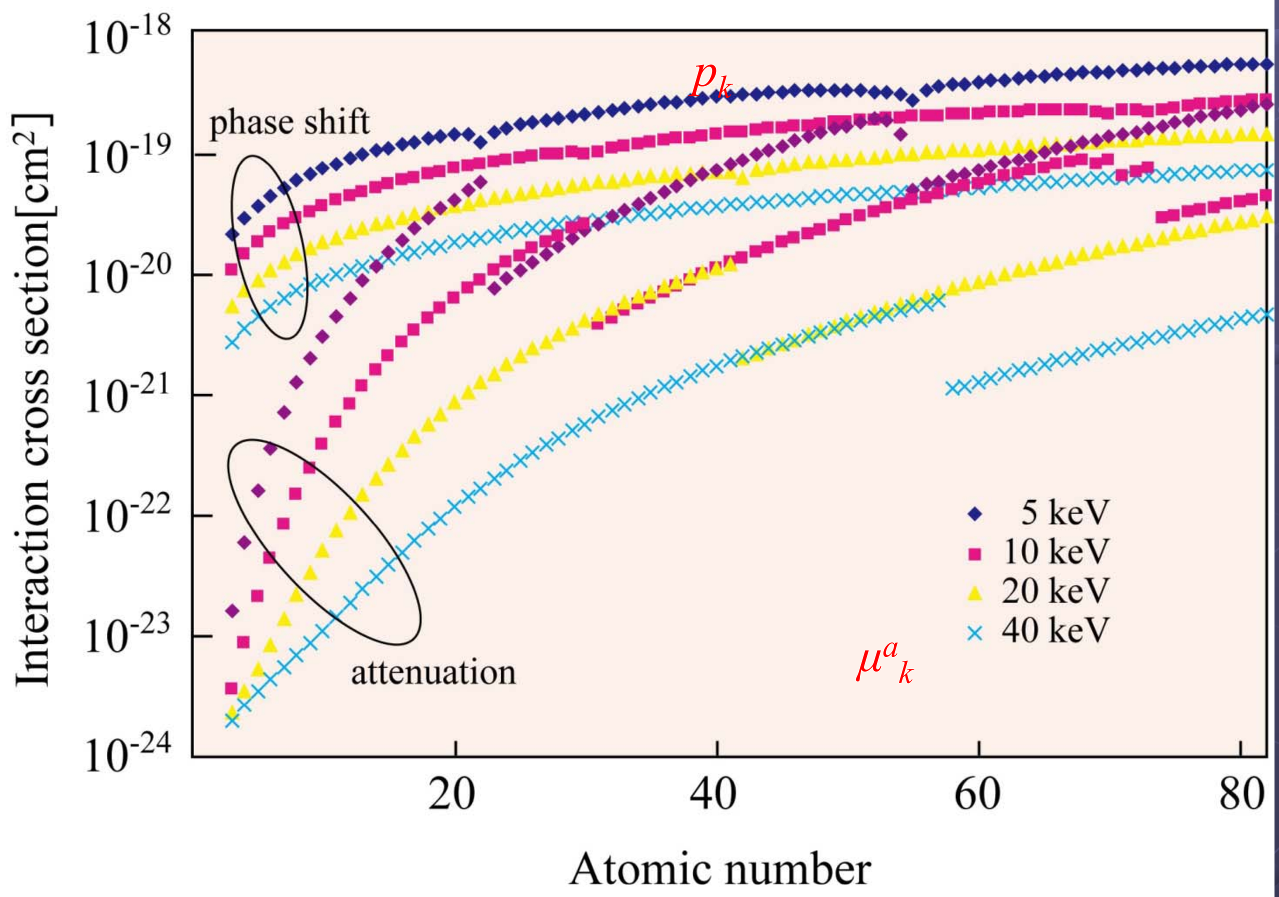

Imaging using phase shift of hard x-rays has much higher sensitivity to materials consisting of light elements!

X-ray phase imaging vs. X-ray absorption imaging

An example of a 1mm-thick slice of rat's cerebellum
（X-ray wavelength：1 Å（12.4keV））

Phase image

Absorption image

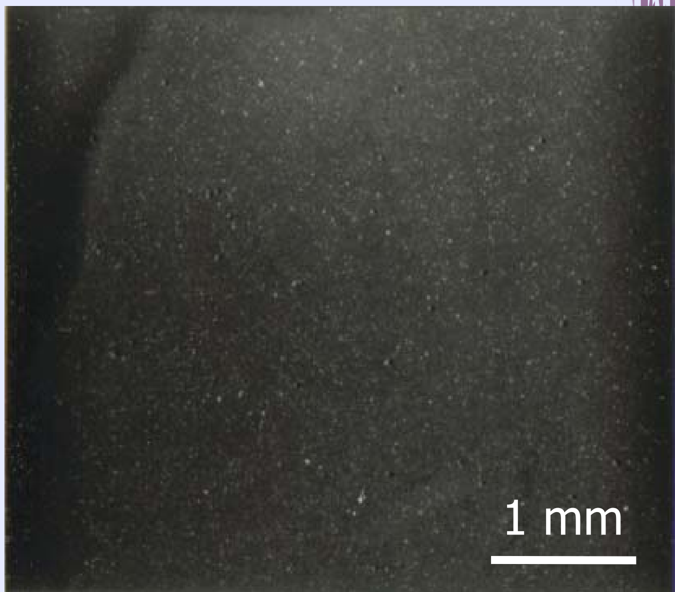

Image obtained by using a X-ray crystal interferometer

A. Momose & J. Fukuda, *Med. Phys.* 1995.

Phase tomogram

@12.4 keV

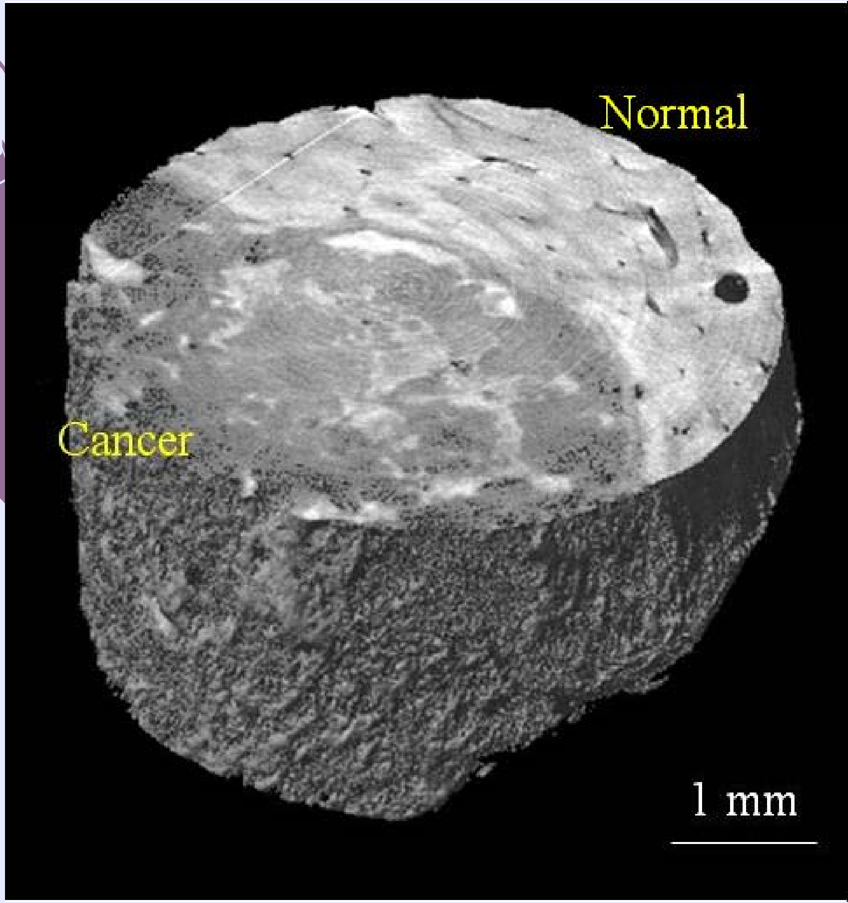

rabbit liver

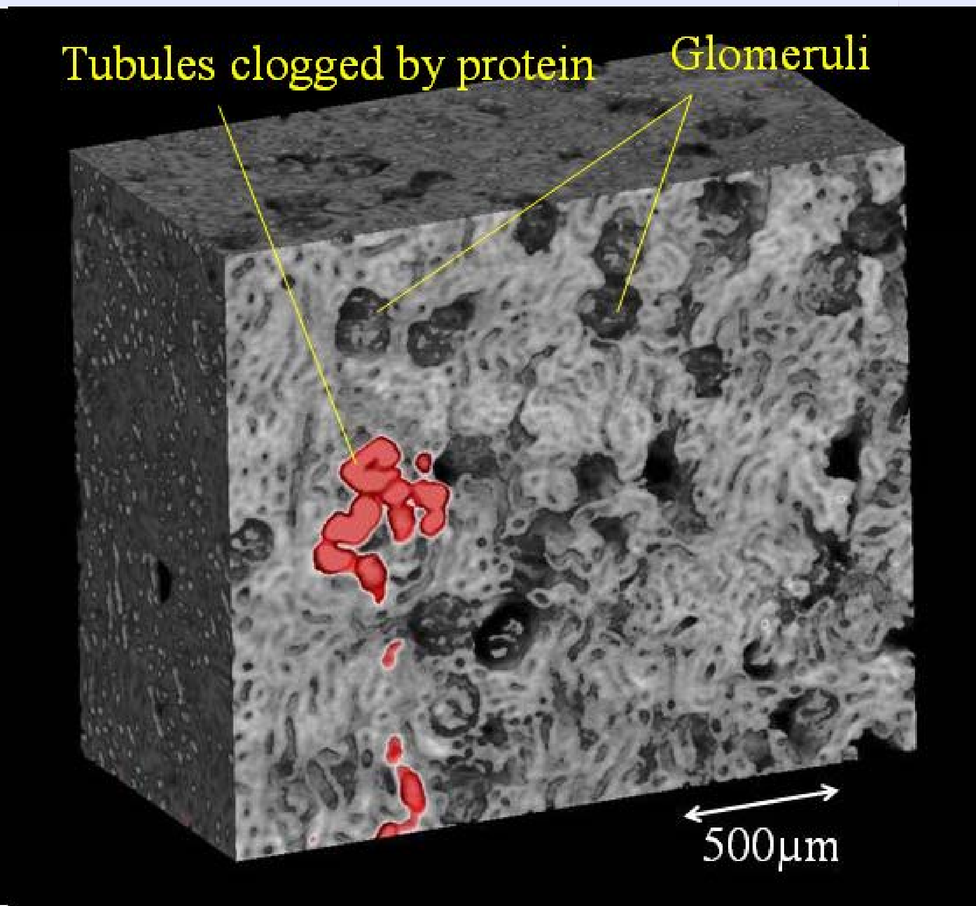

rat kidney

Mouse tail

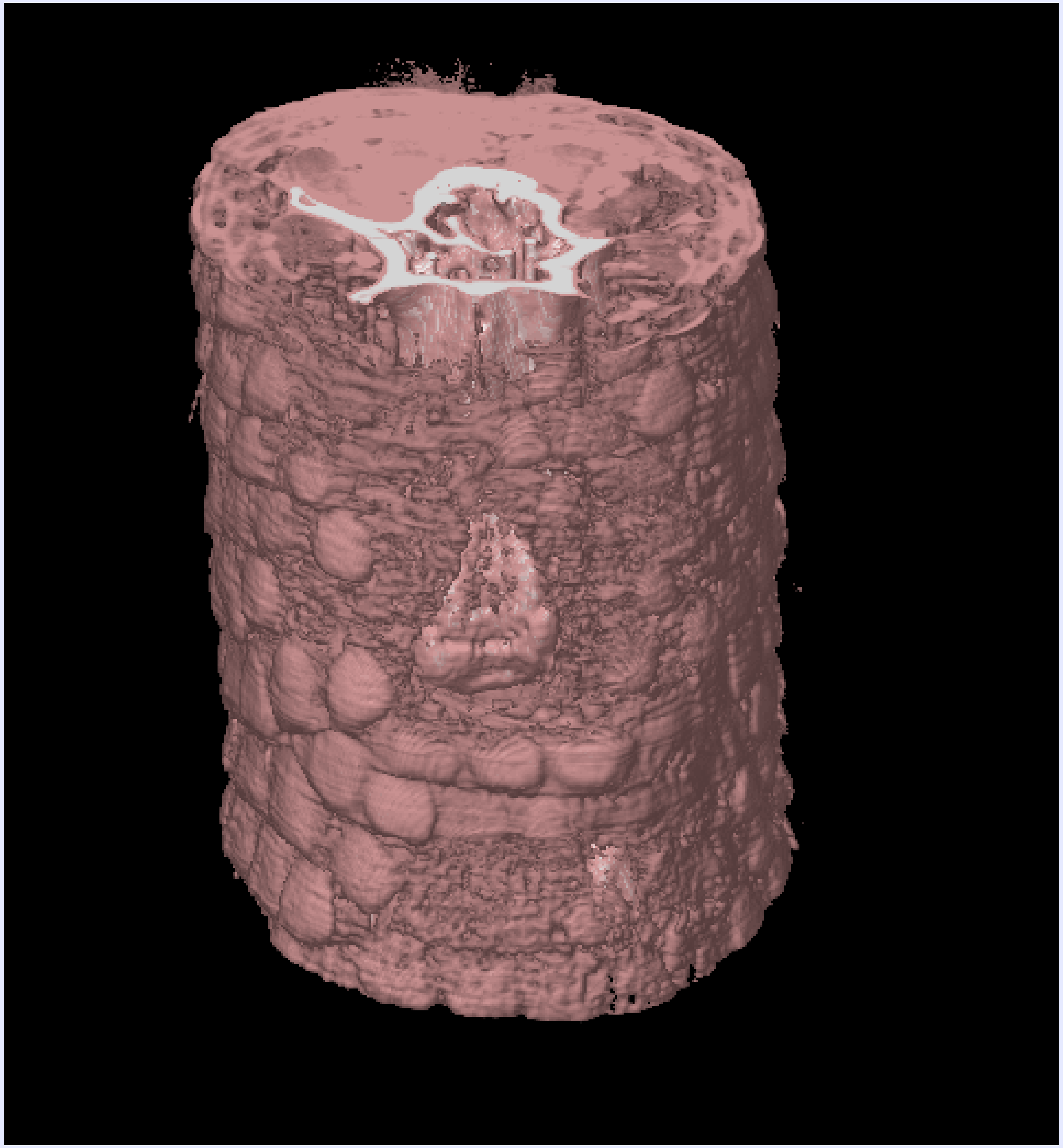

How X-ray phase shift is converted to intensity modulation?

Phase information is lost by simple intensity measurement

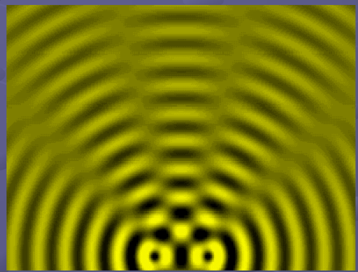

- interference

- Fresnel diffraction

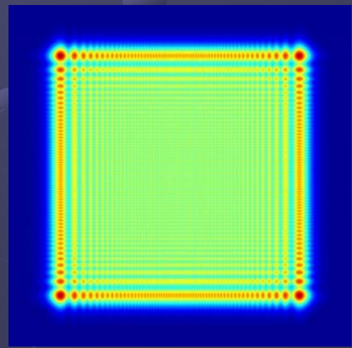

- refraction

Techniques for X-ray phase imaging

Tow-beam interferomrtry

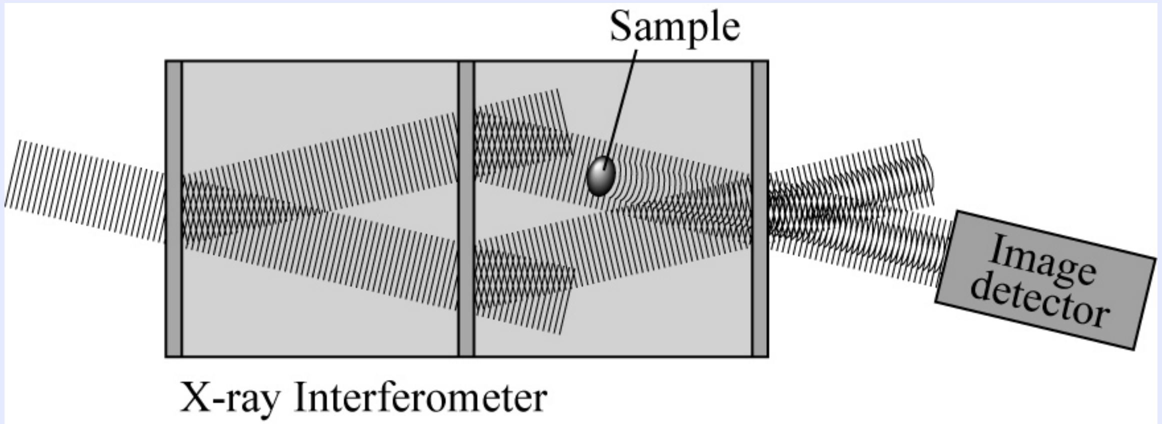

Principle of X-ray Phase Tomography — Obtaining a Fringe Image

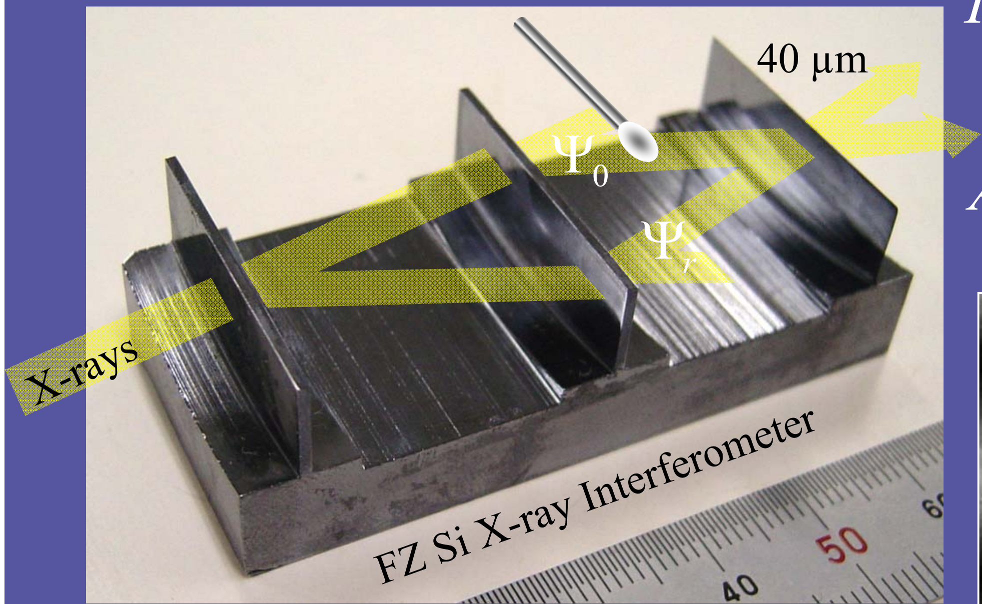

$$I = \left|\Psi_o + \Psi_r\right|^2$$

$$= A + B\cos\left[\Phi(x,y) + \Delta(x,y)\right]$$

A : average intensity $\quad B$: fringe contrast

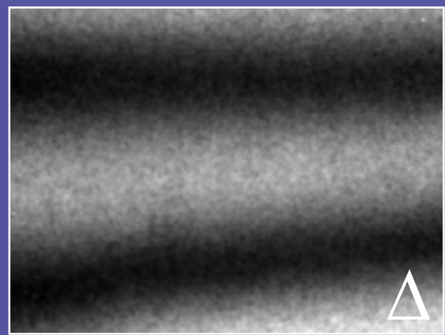

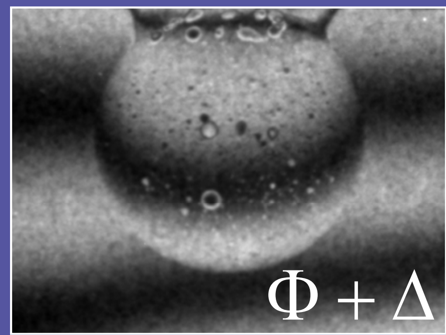

Principle of X-ray Phase Tomography — Fringe Scanning Method

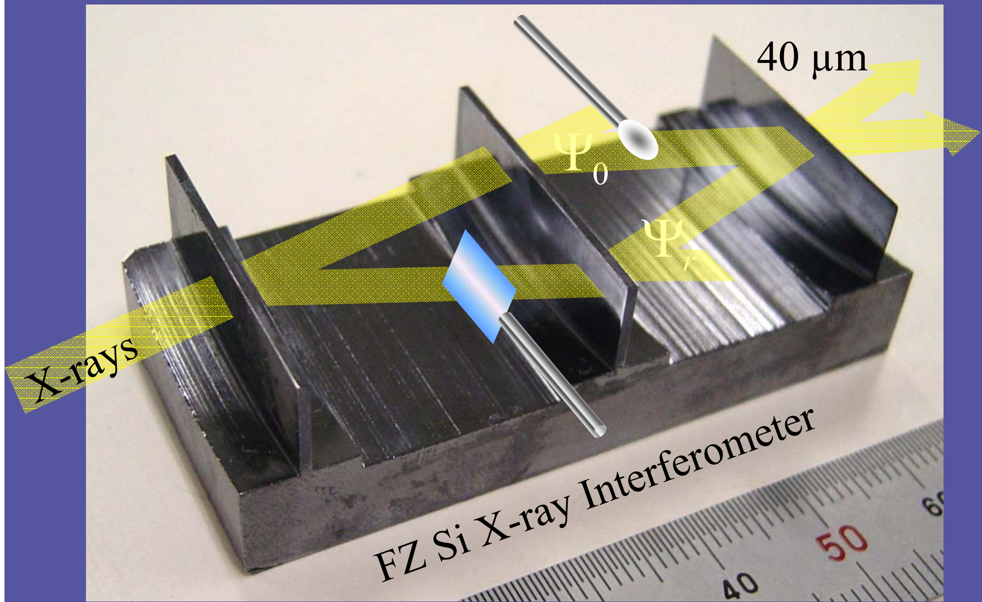

$$I_k = \left|\Psi_o + \Psi_r\right|^2$$
$$= A + B\cos(\Phi + \Delta + 2\pi k / M)$$
$$k = 1, 2 \cdots, M$$

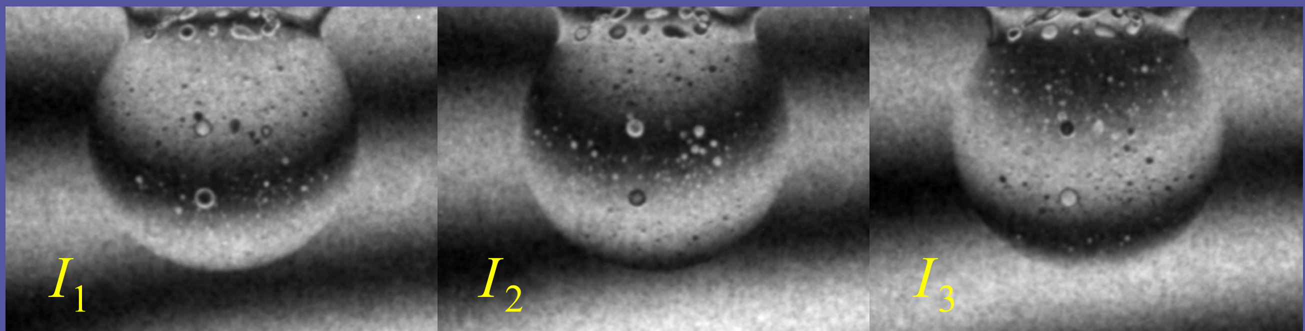

$\cdots$ I_M

Principle of X-ray Phase Tomography — Unwapping

$$\Phi + \Delta = \arg\left[\sum_{k=1}^{M} I_k \exp\left(-2\pi i \frac{k}{M}\right)\right]$$

$$= \tan^{-1}\left(\frac{I_2 - I_4}{I_1 - I_3}\right) \quad \text{when} \quad M = 4.$$

Phase unwrapping

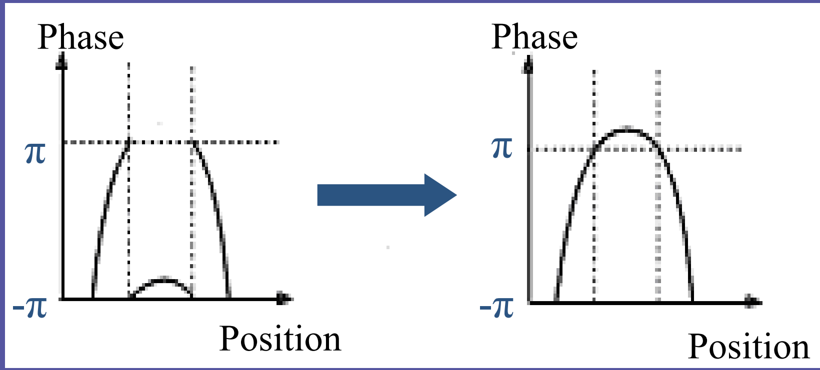

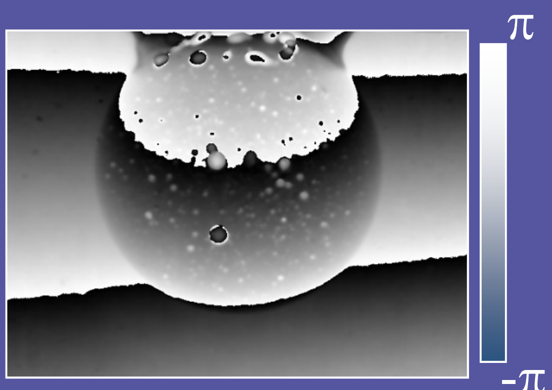

Wrapped phase map

Unwrapped phase map

Repeating this measurement at plural angular positions of sample rotation, a phase tomogram is reconstructed.

Propagation-based method

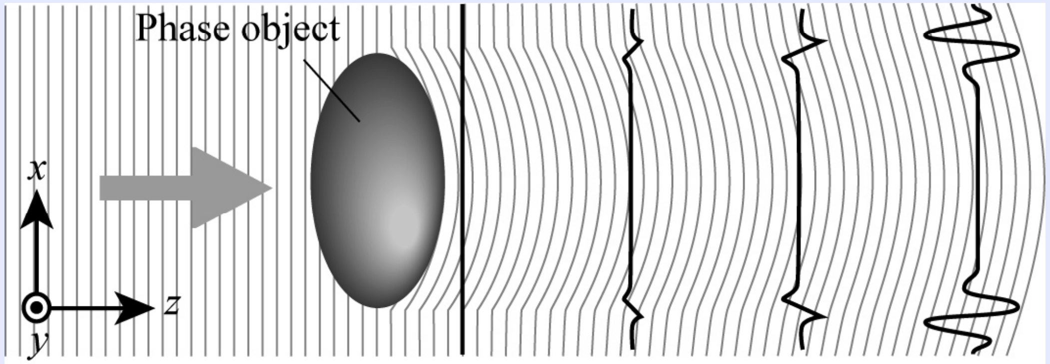

Intensity generated downstream of objects (simulation)

Ideal absorber
(red: zero transmission)

Pure phase object
(blue: phase shift π)

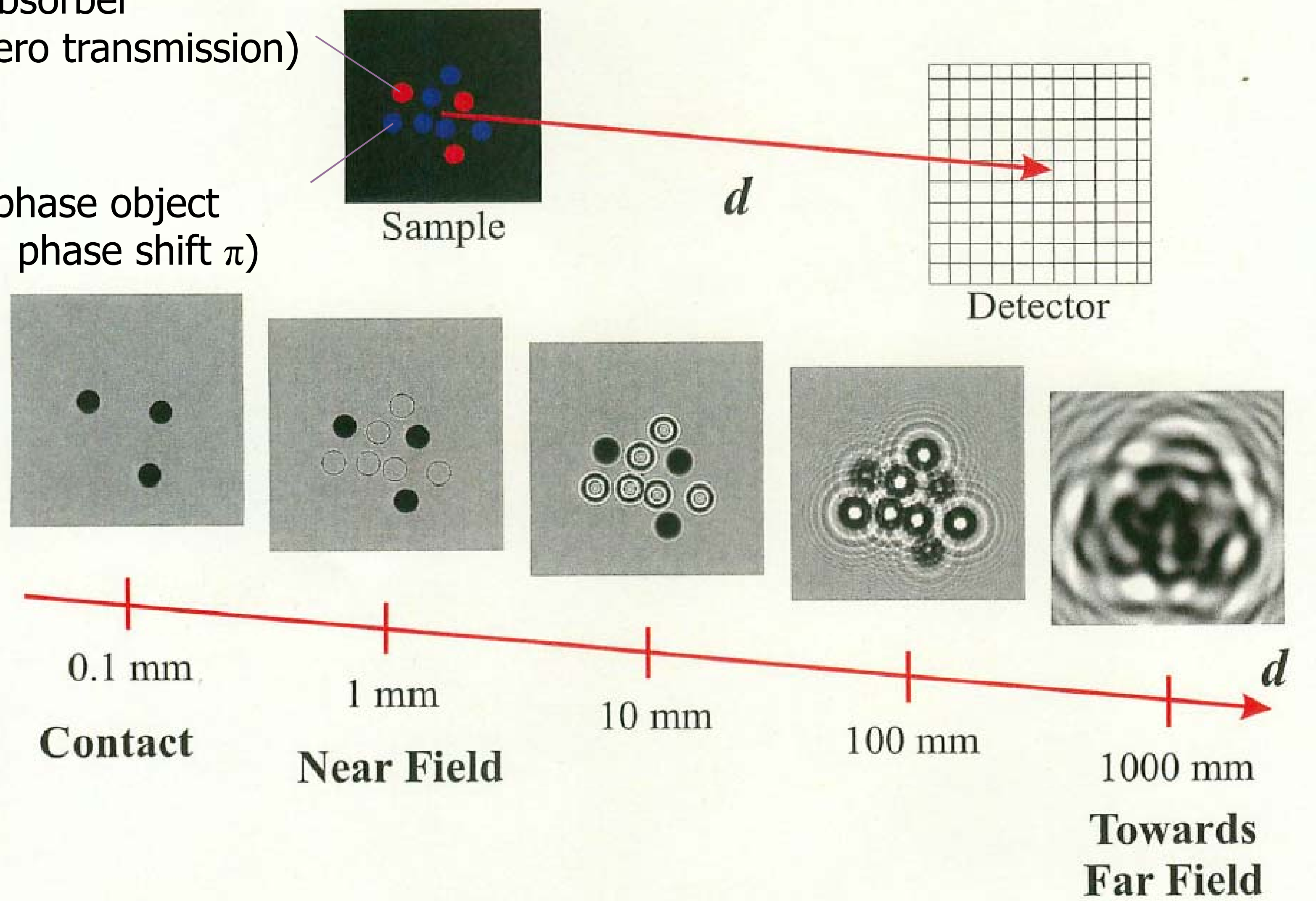

J. Als-Nielsen & D. McMorrow, "Elements of Modern X-ray Physics", 2nd ed. (2011).

Spatial coherence & van Cittert-Zernike theorem

Perfect (spatially) coherent beam

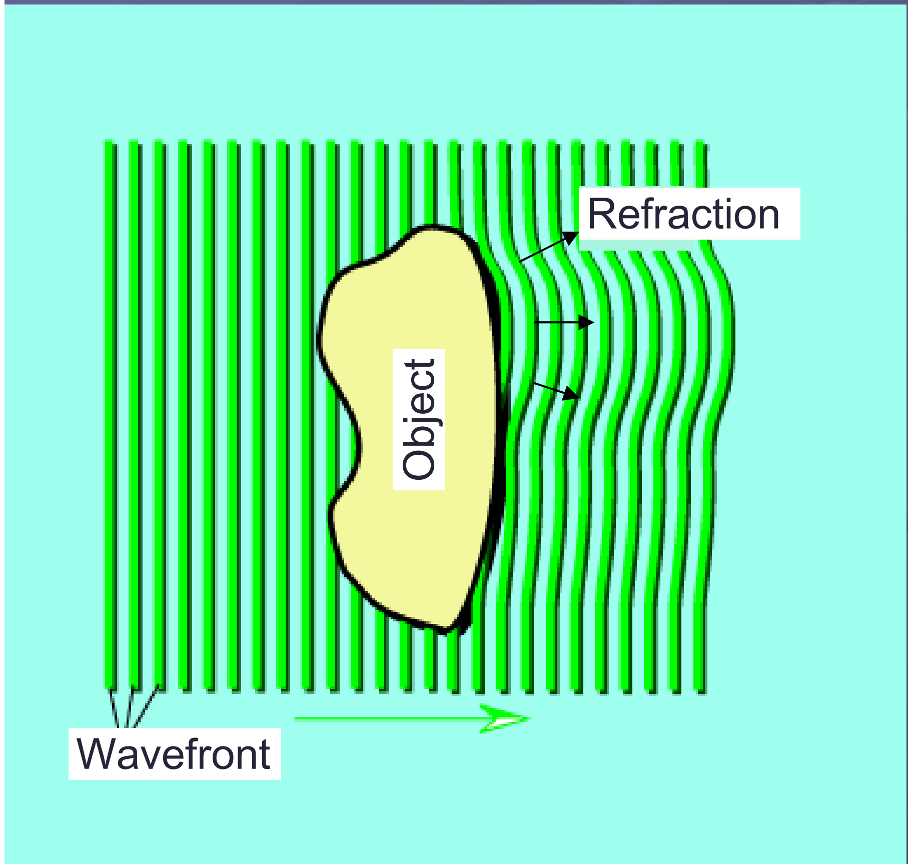

Partially coherent beam

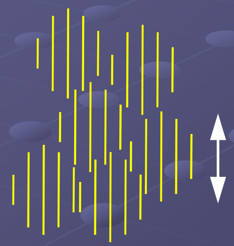

spatial coherence length: L

$$L \sim \lambda/(2\pi\Delta\theta)$$

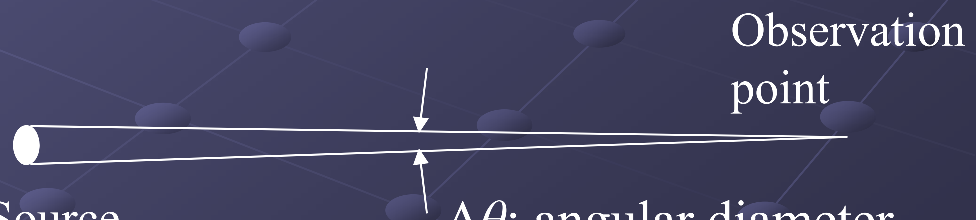

$\Delta\theta$: angular diameter of source at the observation point

Nude mouse

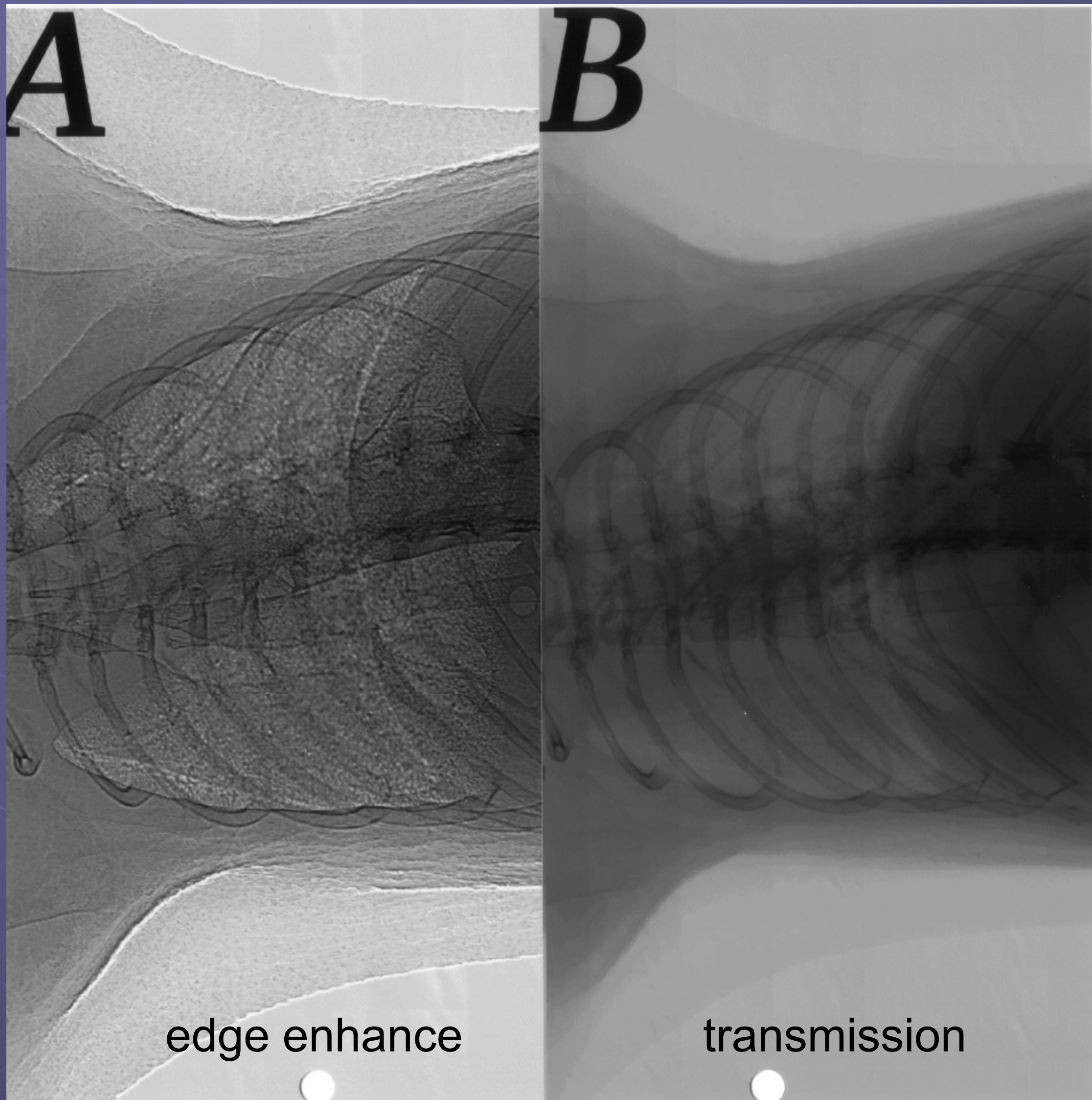

N. Yagi *et al. Med. Phys.* **26** (1999) 2190.

Analyzer-based method with crystal

Diffraction-Enhanced Imaging (DEI)

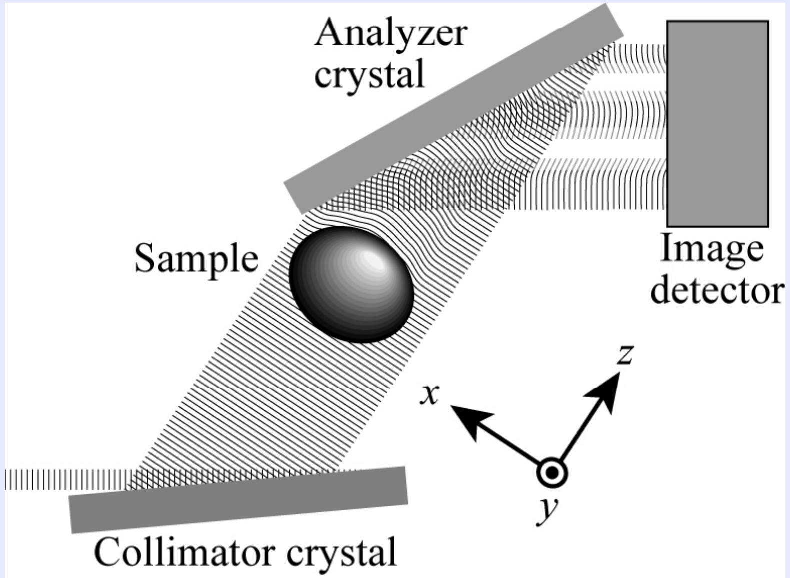

How about detecting beam deflection caused by refraction?

refractive index： $1 - \delta$ $\delta \sim 10^{-6}$

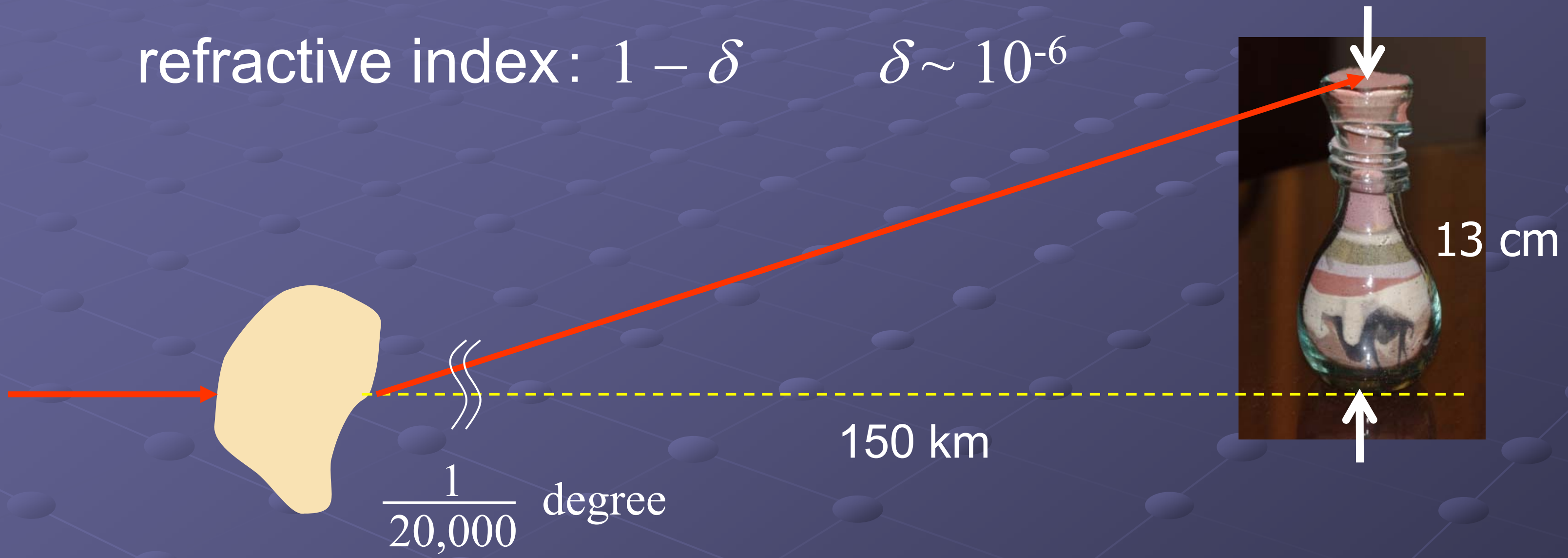

Days Inn Hotel
@Amman

@Petra

Direct detection of X-ray beam deflection is not easy!

Analyzer-based method

20.7 keV SR

ant

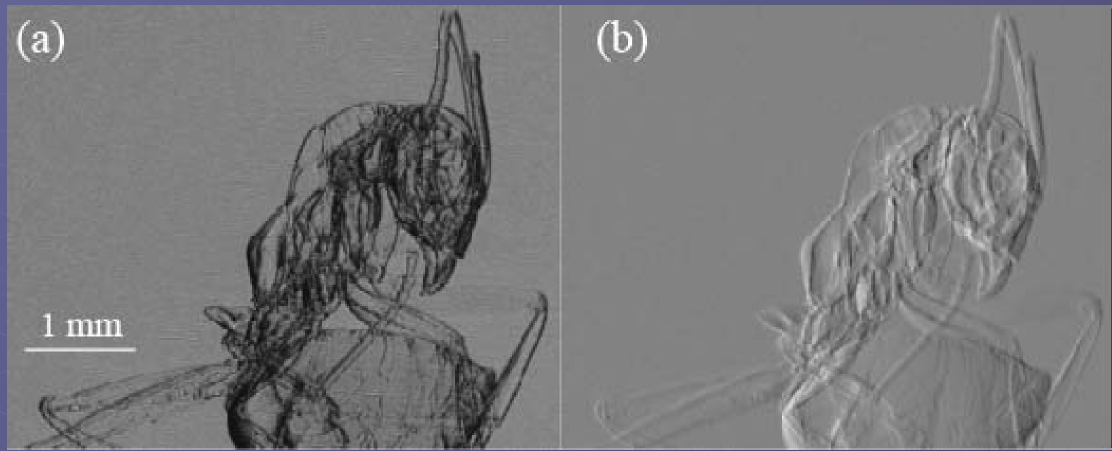

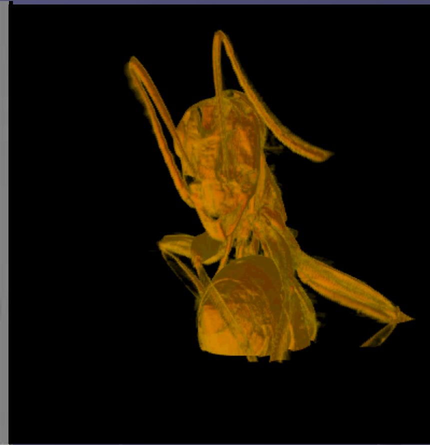

I. Koyama et al.,
AIP Proc. **705** (2004) 1283.

Diffraction enhanced image (DEI) | Image mapping X-ray refraction | Phase tomogram

mouse tail

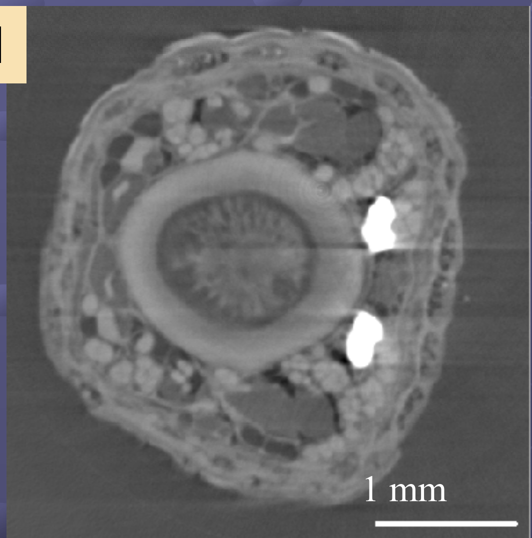

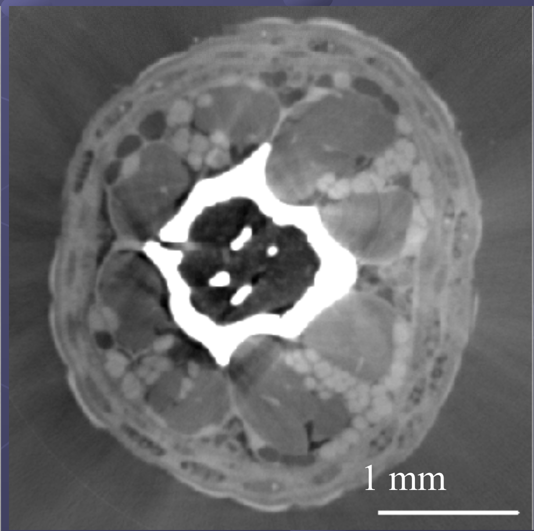

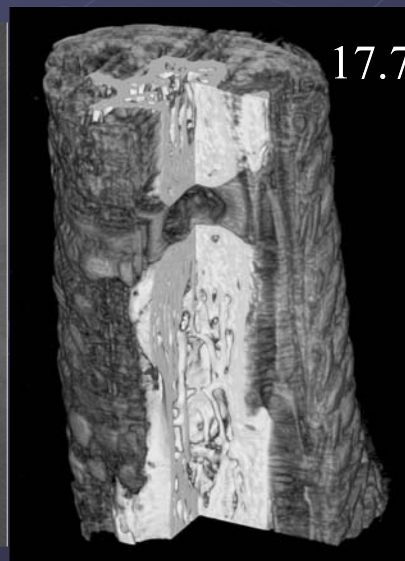

17.7 keV SR

I. Koyama et al., *Jpn. J. Appl. Phys* **44** (2005) 8219.

Analyzer-based method with transmission gratings

Talbot Interferometry

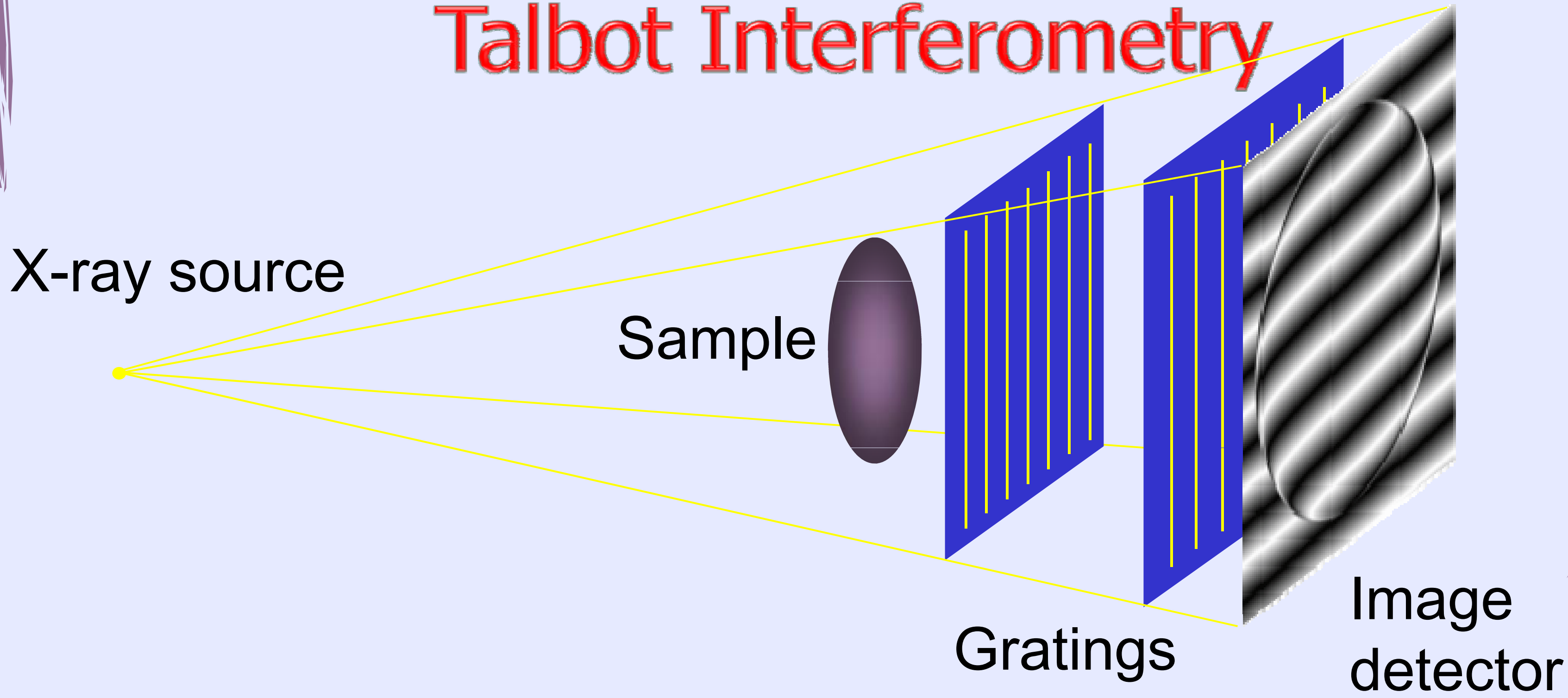

X-ray Talbot interferometer

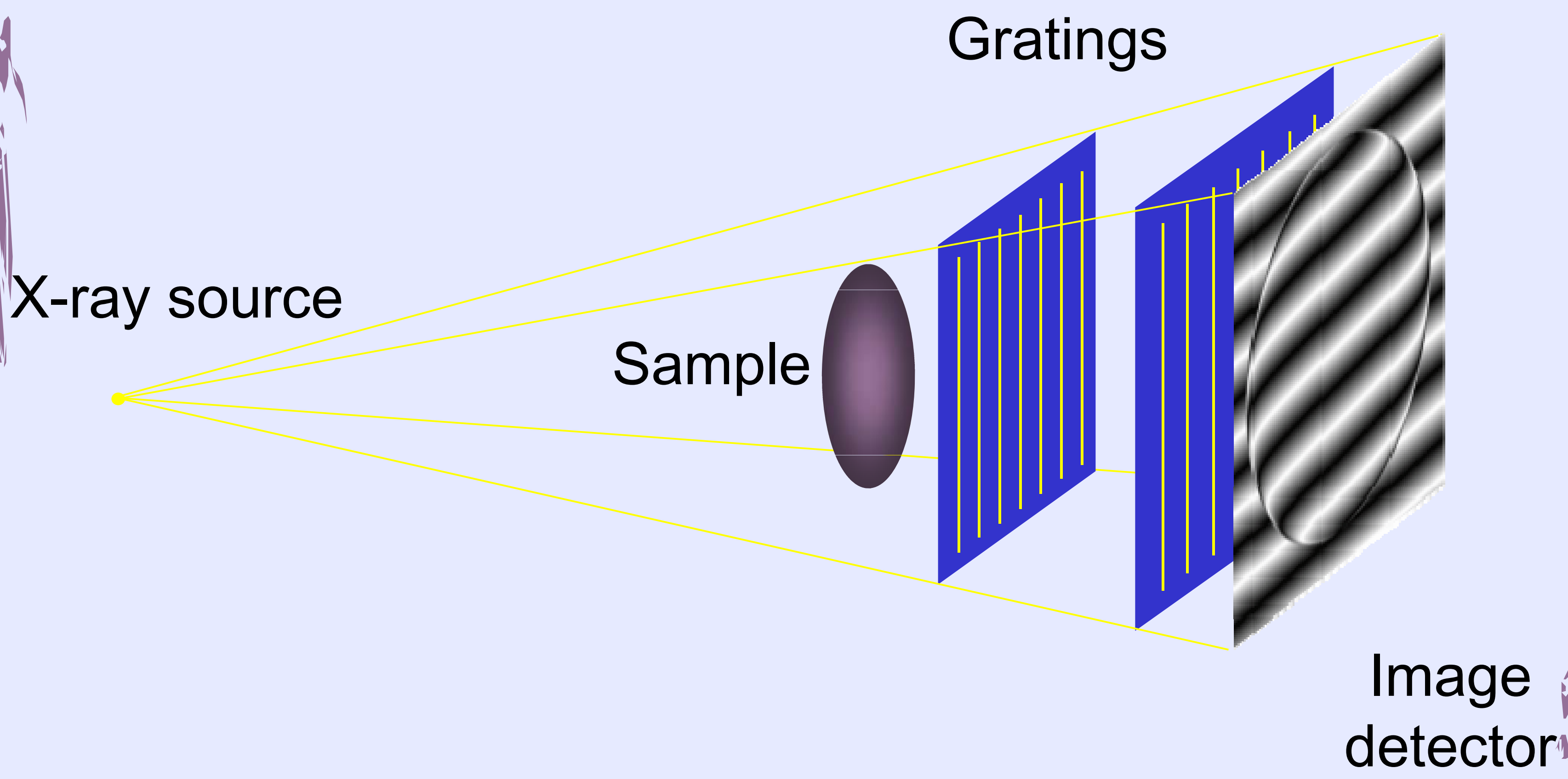

Talbot Effect – a self-imaging phenomenon

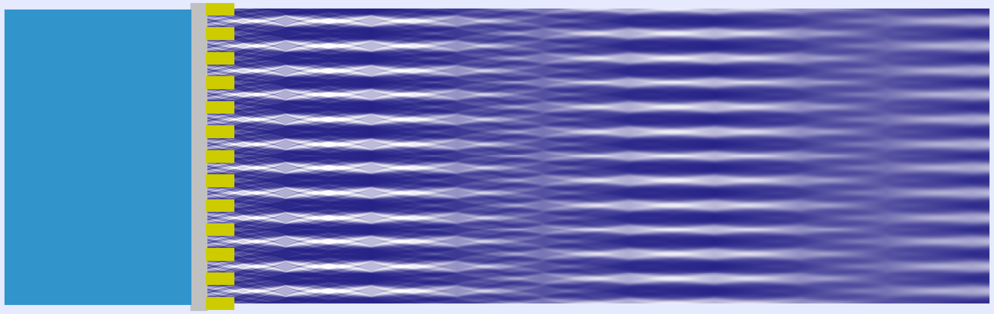

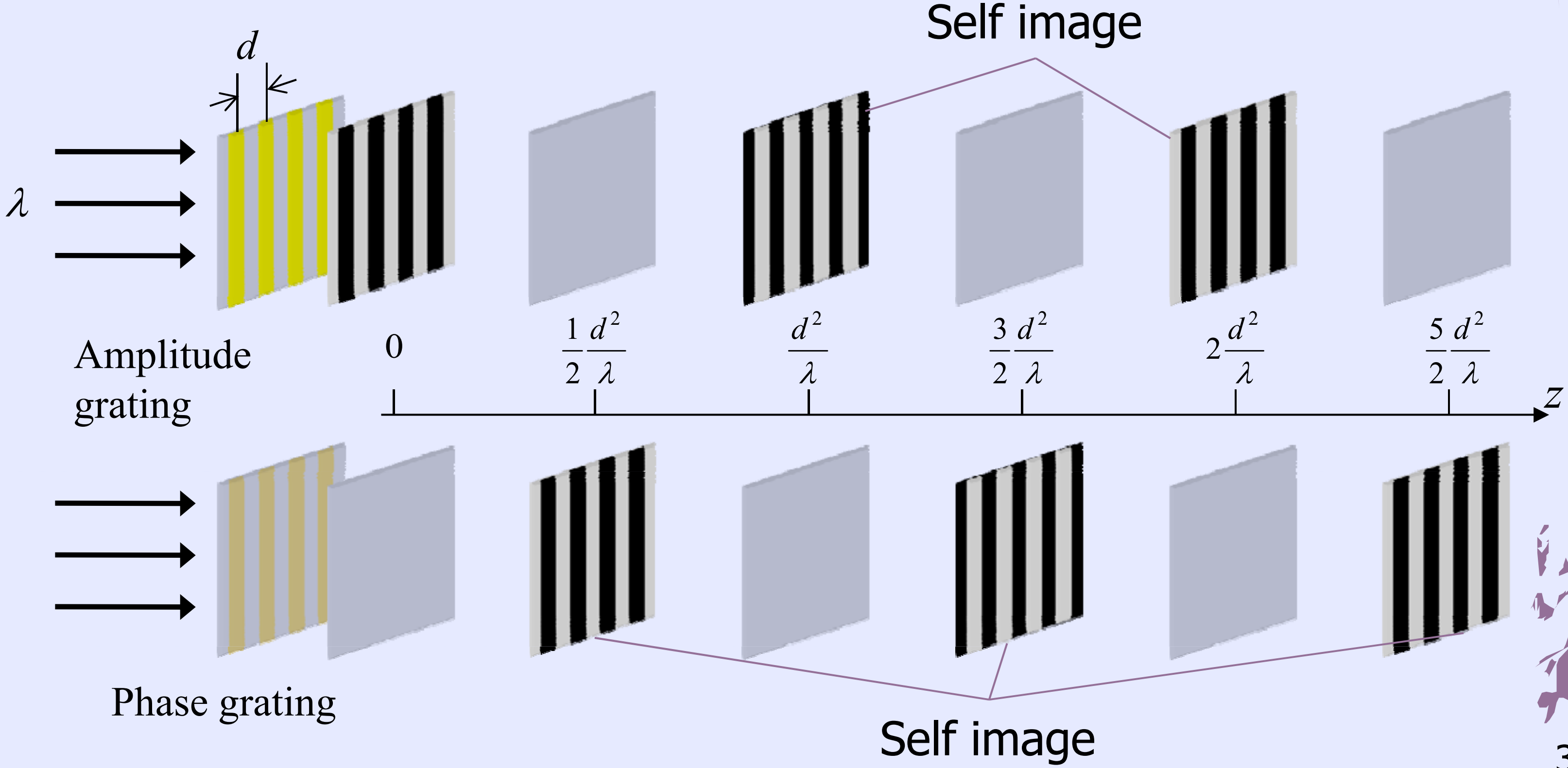

Talbot Interferometer

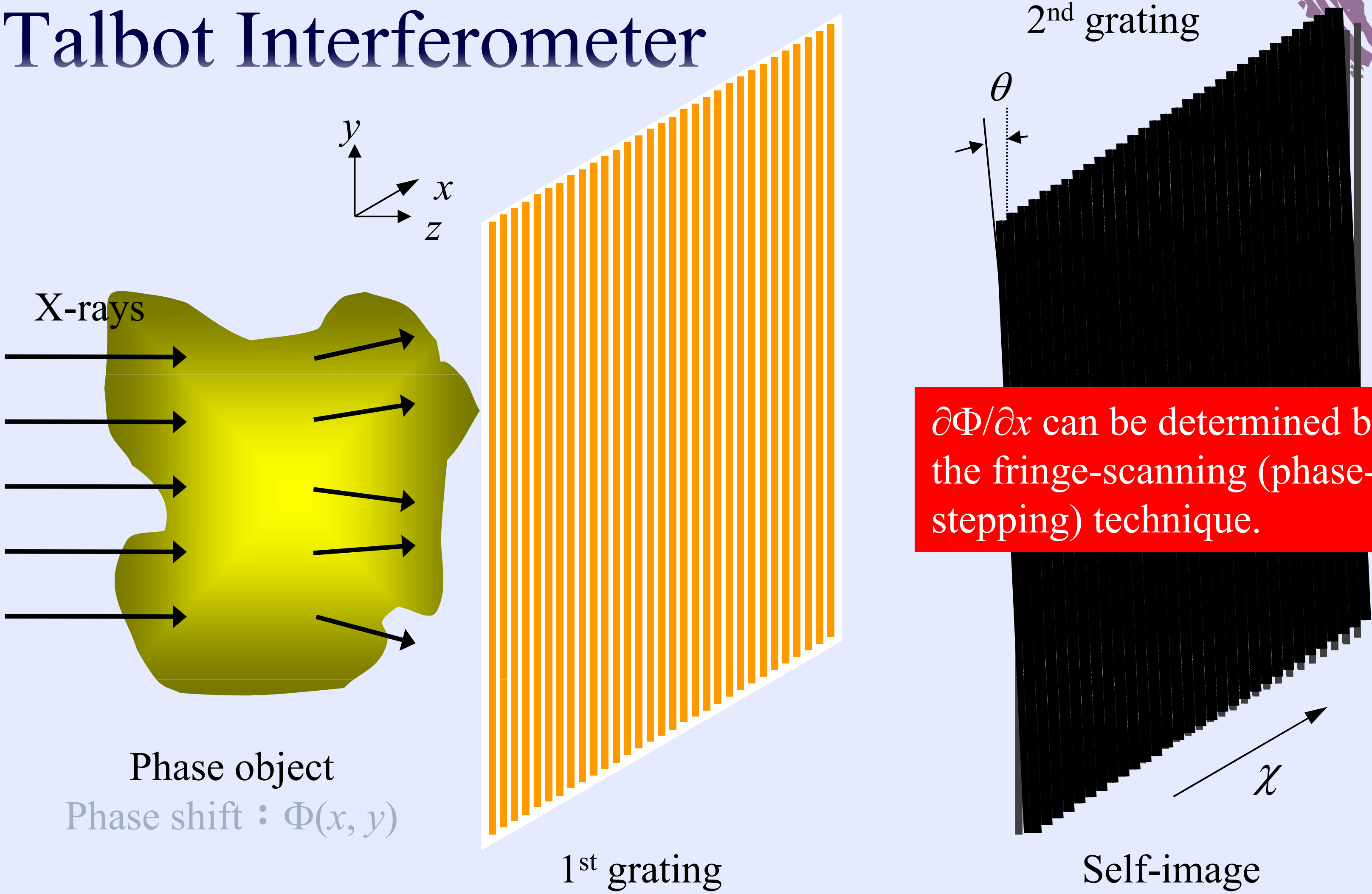

∂Φ/∂x can be determined by the fringe-scanning (phase-stepping) technique.

Moiré pattern　Deformed self-image

$$I(x, y.\sum_n b_n \exp\left[i2\pi \frac{nx}{d}\right] \Rightarrow \sum_n b_n \exp\left[i2\pi \frac{n}{d}\left(x - z\frac{\partial \Phi}{\partial x}\right)\right]$$

How to obtain phase image and tomogram

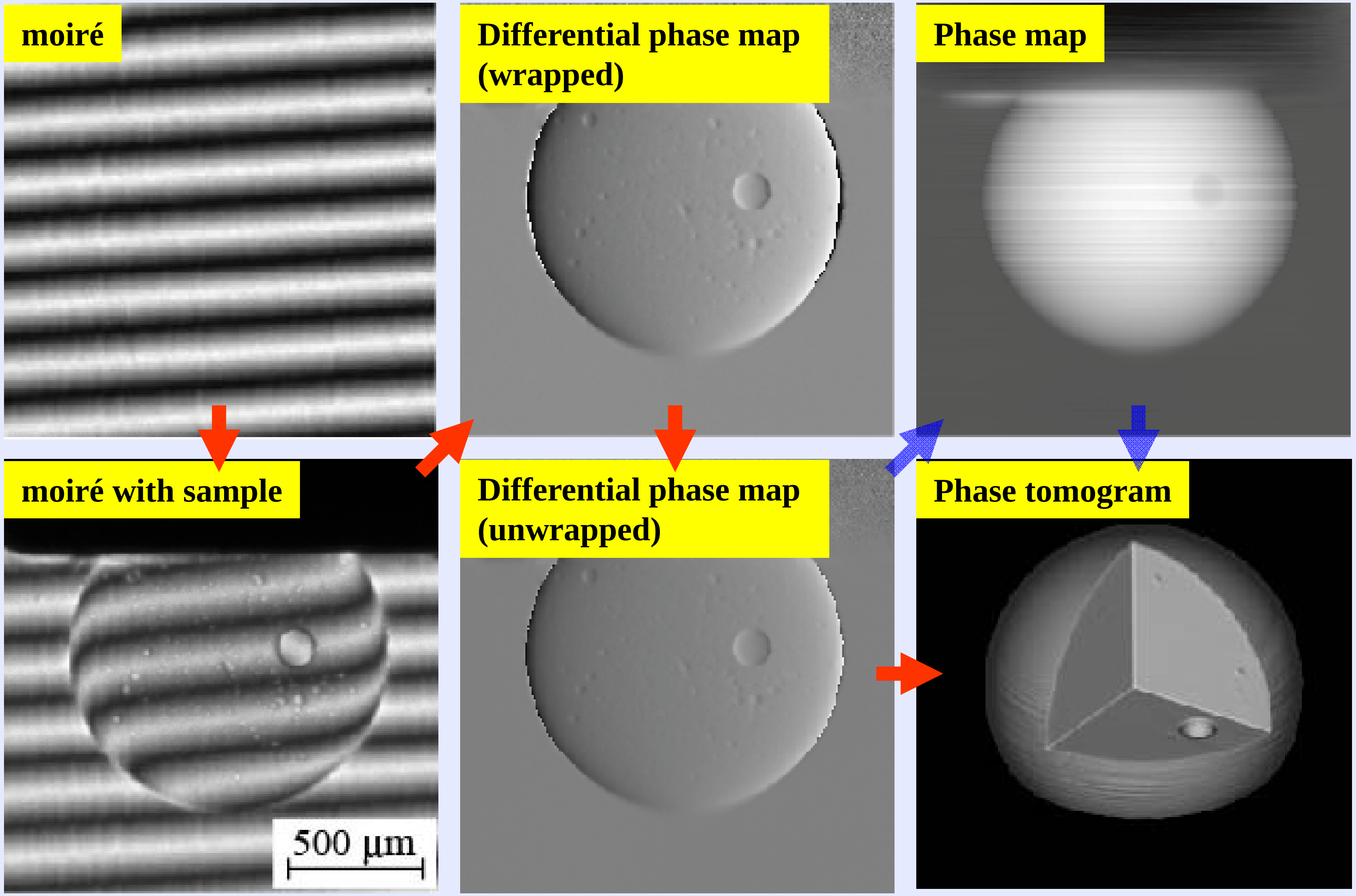

Three images obtained by X-ray Talbot interferometer

Fringe scanning method

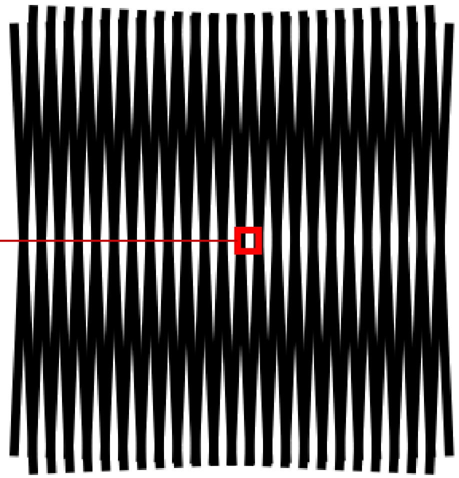

Intensity at a pixel

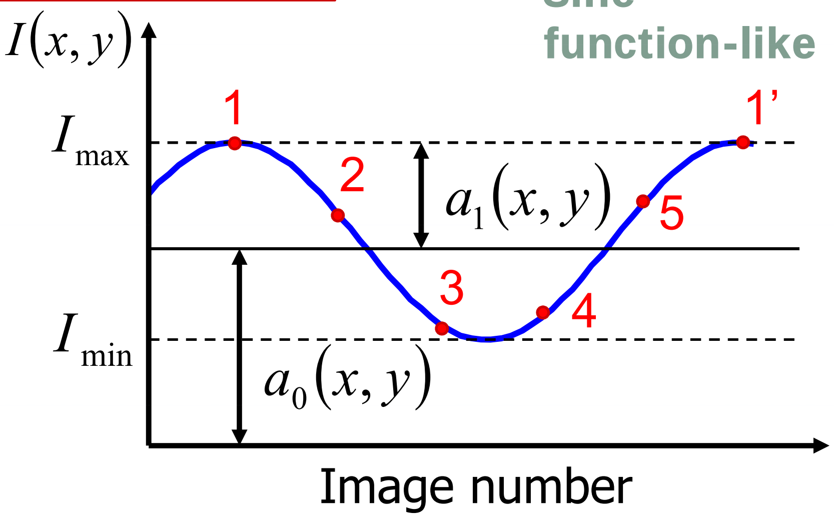

Absorption image

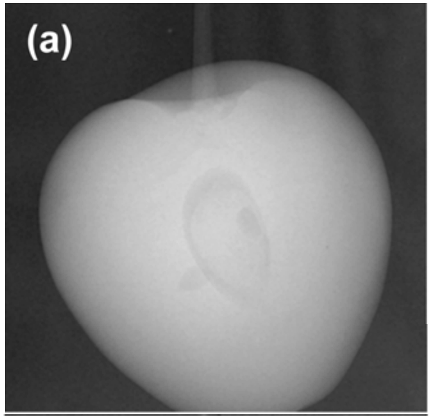

Differential phase image

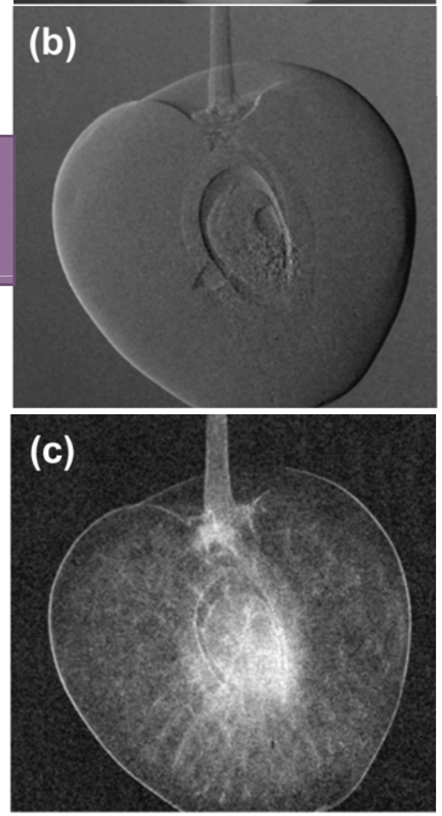

Visibility contrast image (ultra-small-angle X-ray scattering imaging)

Advantages of X-ray Talbot interferometry

- Setup is simple.
- Large area (100 mm×100 mm) imaging is possible.
- Wide energy band width is available.
- Spherical wave is available.
- Wide working space can be used for the sample.
- Incoherent X-ray source is available (Talbot-Lau type).

Using compact laboratory source ↓ Medical application	Using white synchrotron radiation source ↓ High speed imaging/tomography	Combining X-ray lens ↓ X-ray imaging microscopy

Observation with Microfocus Source

Microfocus X-ray tube （focus ~ 8 μm）
W target : 50kV, 120 μA
Exposure : 100 min.

Hamamatsu Photonics
L9181S

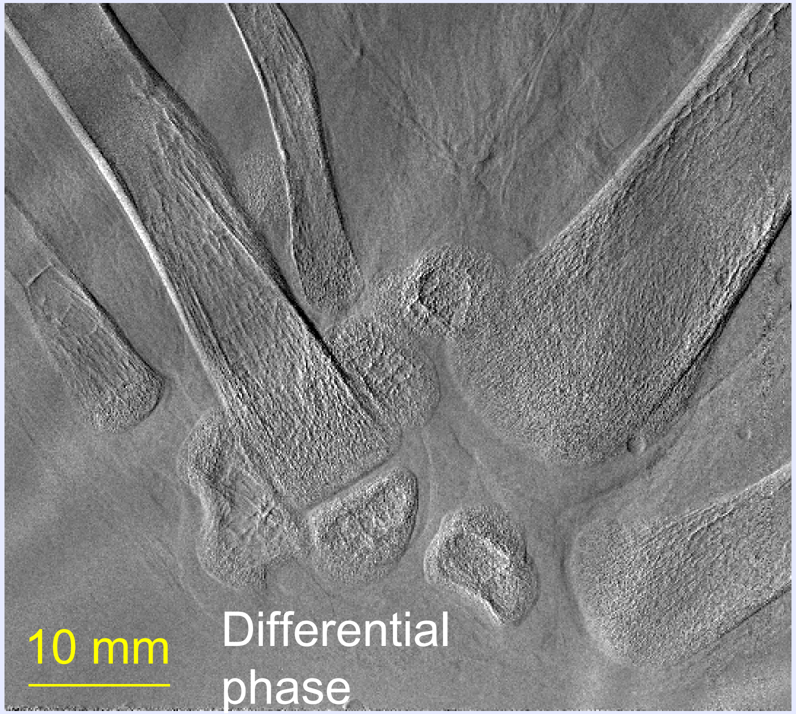

※observed in water

confidential

High-speed X-ray phase imaging with white synchrotron beam

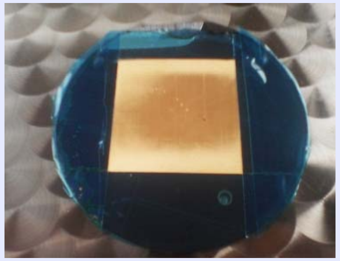

X-ray grating

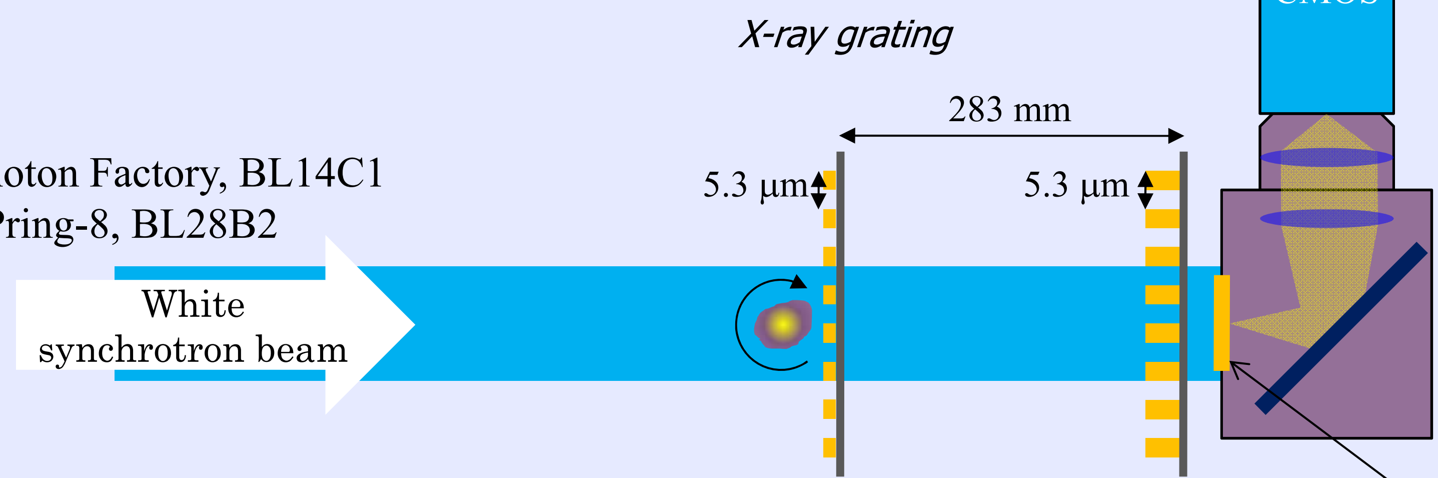

confidential

4DCT

4DCT (irradiation effect)
Sample: glue (Scotch（3M）)

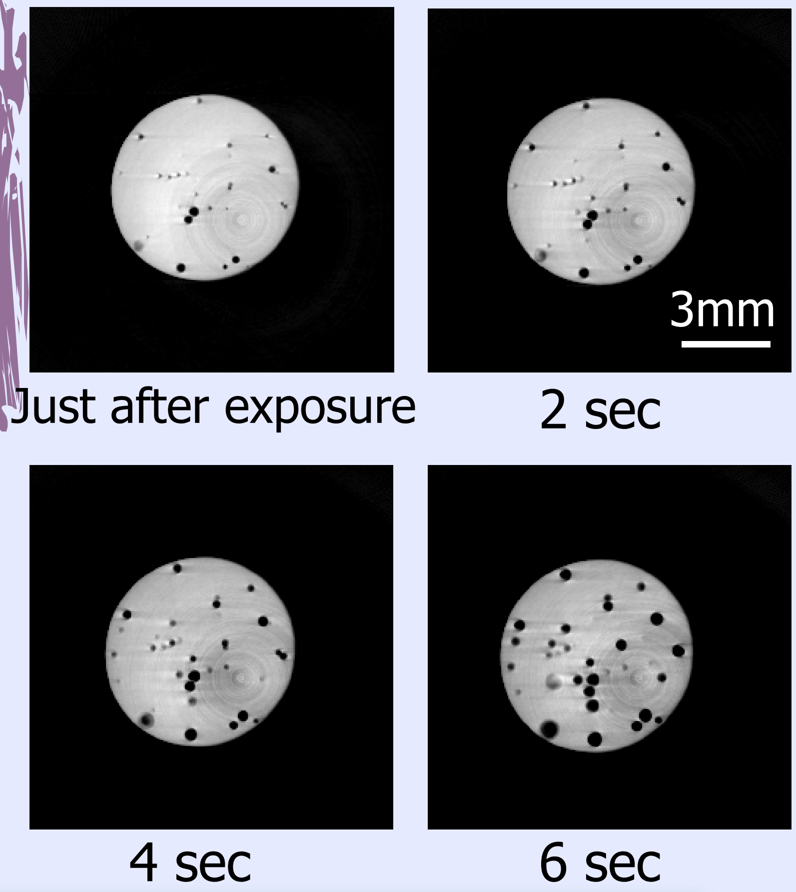

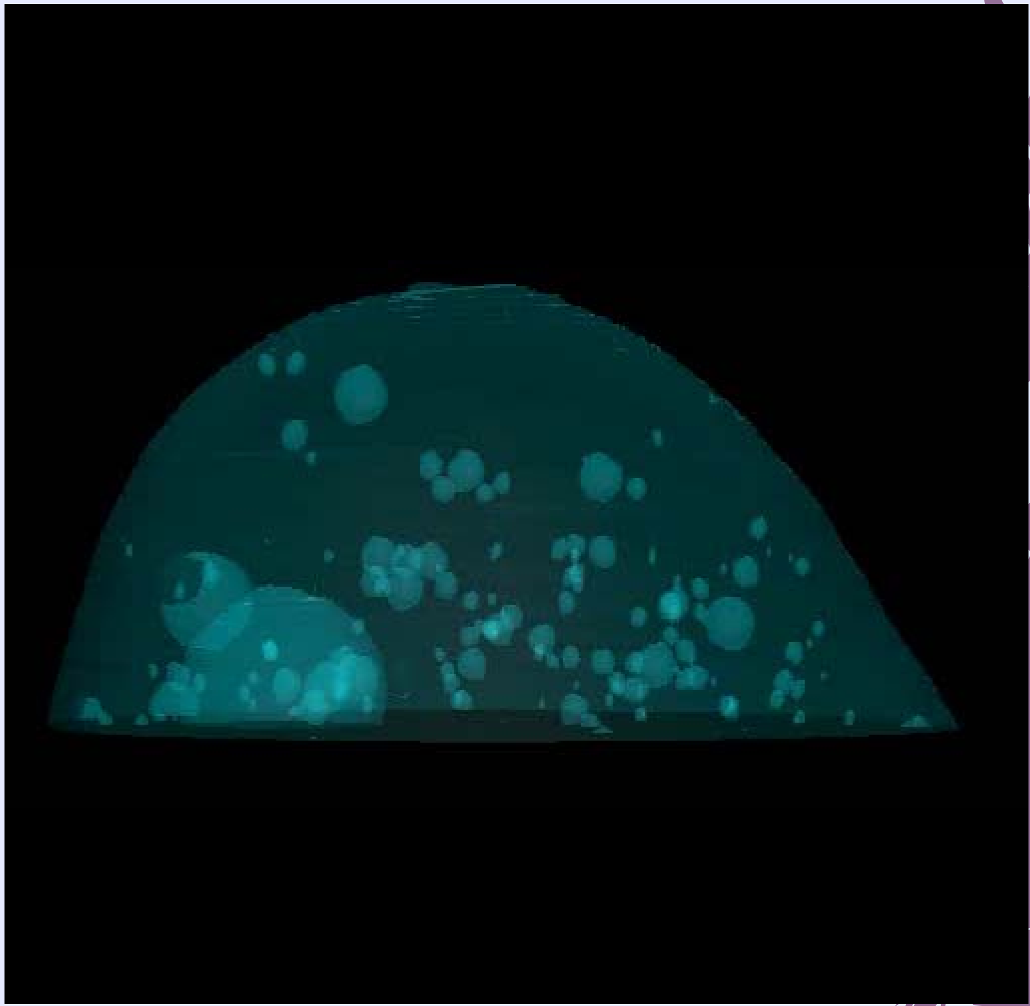

Exposure time: 1 ms/frame
0.25 sec/180 deg

X-ray microscopy – image forming method

Optical systems for Image-forming | **Signals**

- Imaging microscopy

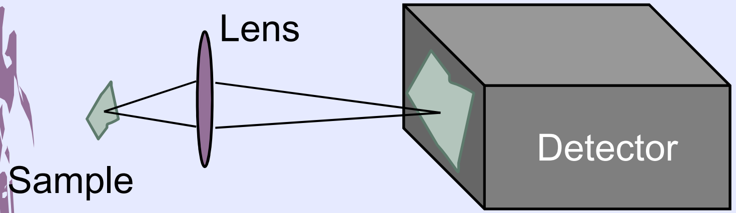

- Scanning microscopy

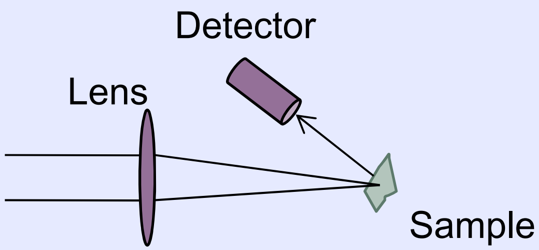

- Diffraction microscopy

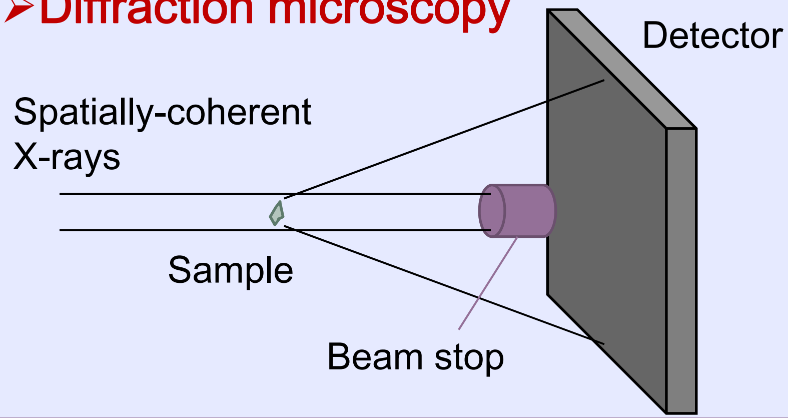

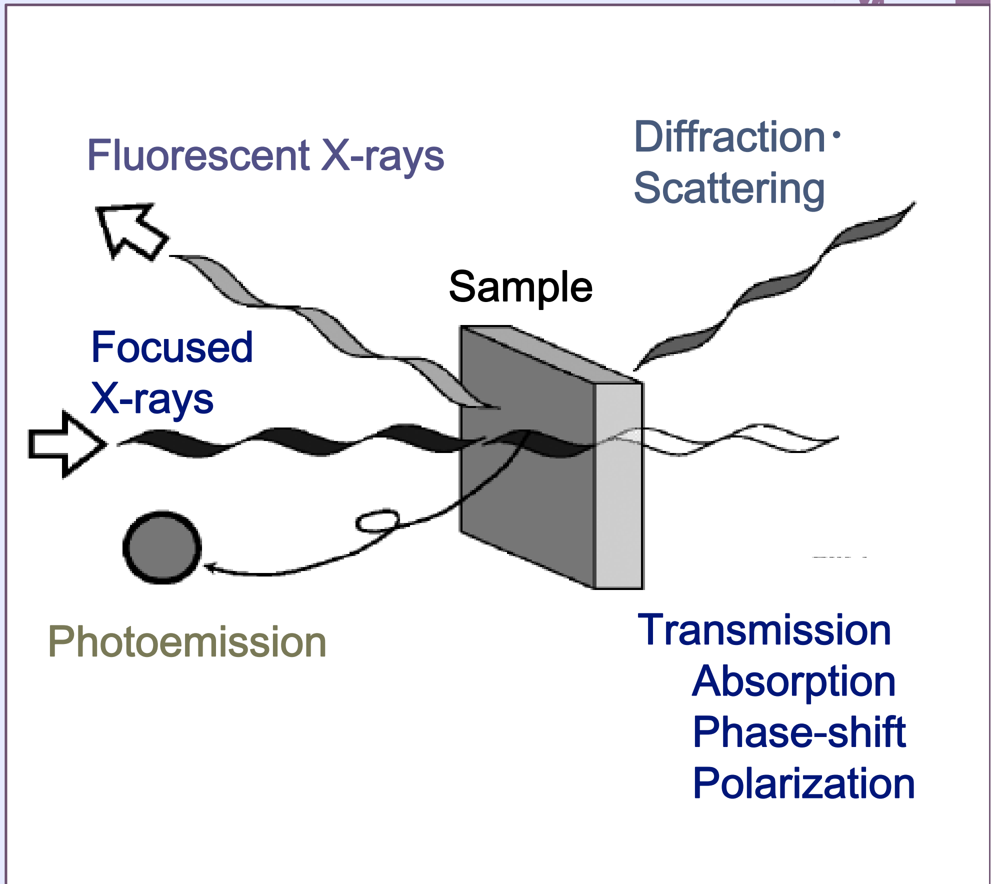

S.Aoki、放射光 23 (2010).

X-ray microscopy – optics

X-ray focusing devices

- Diffraction e.g., Fresnel zone plate (FZP)

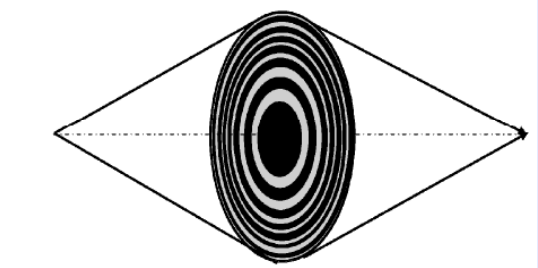

- Refraction e.g., Compound refractive lenses

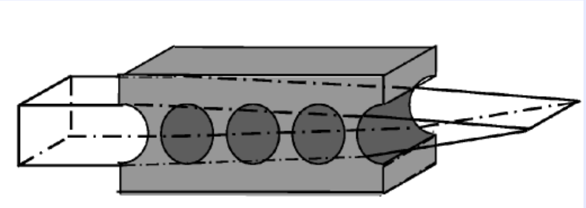

- Reflection e.g., Kerkpatrick-Baez (KB) mirror

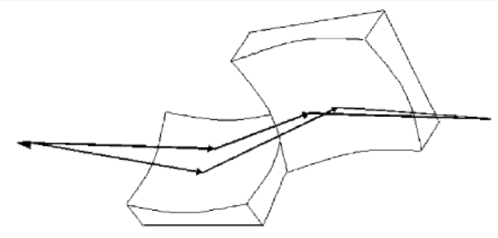

Recent progress in X-ray focusing devices

Figures from 放射光ビームライン光学技術入門（日本放射光学会(2008).

	X-ray optics	Focus size, focal length (X-ray energy, year)	Range of X-ray energy	Aberration		
				Coma	Chromatic	Shape Erorr
Diffraction Type	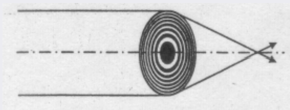 Fresnel zone plate (FZP)	30 nm, f = 80 mm (8keV, 2005)	Soft X-rays Hard X-rays	Small	Yes	Small
	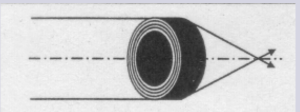 Sputter-Slice FZP	300 nm, f = 220 mm (12.4 keV, 2002)	8-100 keV	Small	Yes	Large
	 Bragg FZP	2.4 μm, f = 700 mm (13.3 keV, 1999)	Hard X-rays	Small	Yes	Small
	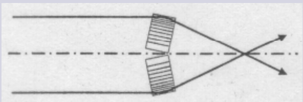 Multi-layer Laue lens	13 nm, f = 1.6 mm (20 keV, 2010)	Hard X-rays	Large	Yes	Small
Refraction Type	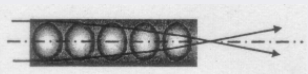 Refractive lens (pressing)	1.6 μm, f = 1.3 m (15 keV, 1999)	Hard X-rays	Small	Yes	Large
	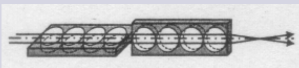 Refractive lens (etching)	47 ×55 nm^2, f = 10 mm (21 keV, 2006)	Hard X-rays	Small	Yes	Small
Reflection Type	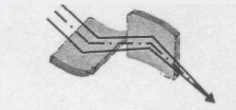 Kirkpatrick-Baez (KB) mirror	7 nm (1D), 11×14 nm^2 (2D), f = 75 mm (20 keV, 2010)	Soft X-rays Hard X-rays	Large	No	Small
	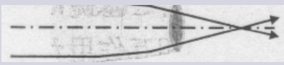 Wolter mirror	700 nm, f = 350 mm (9 keV, 2001)	<10 keV	Small	No	Large
	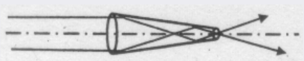 Wave guide	33×69 nm^2 (12.8 keV, 2002)	Soft X-rays Hard X-rays	Large	No	Large

Recent progress in X-ray focusing technology

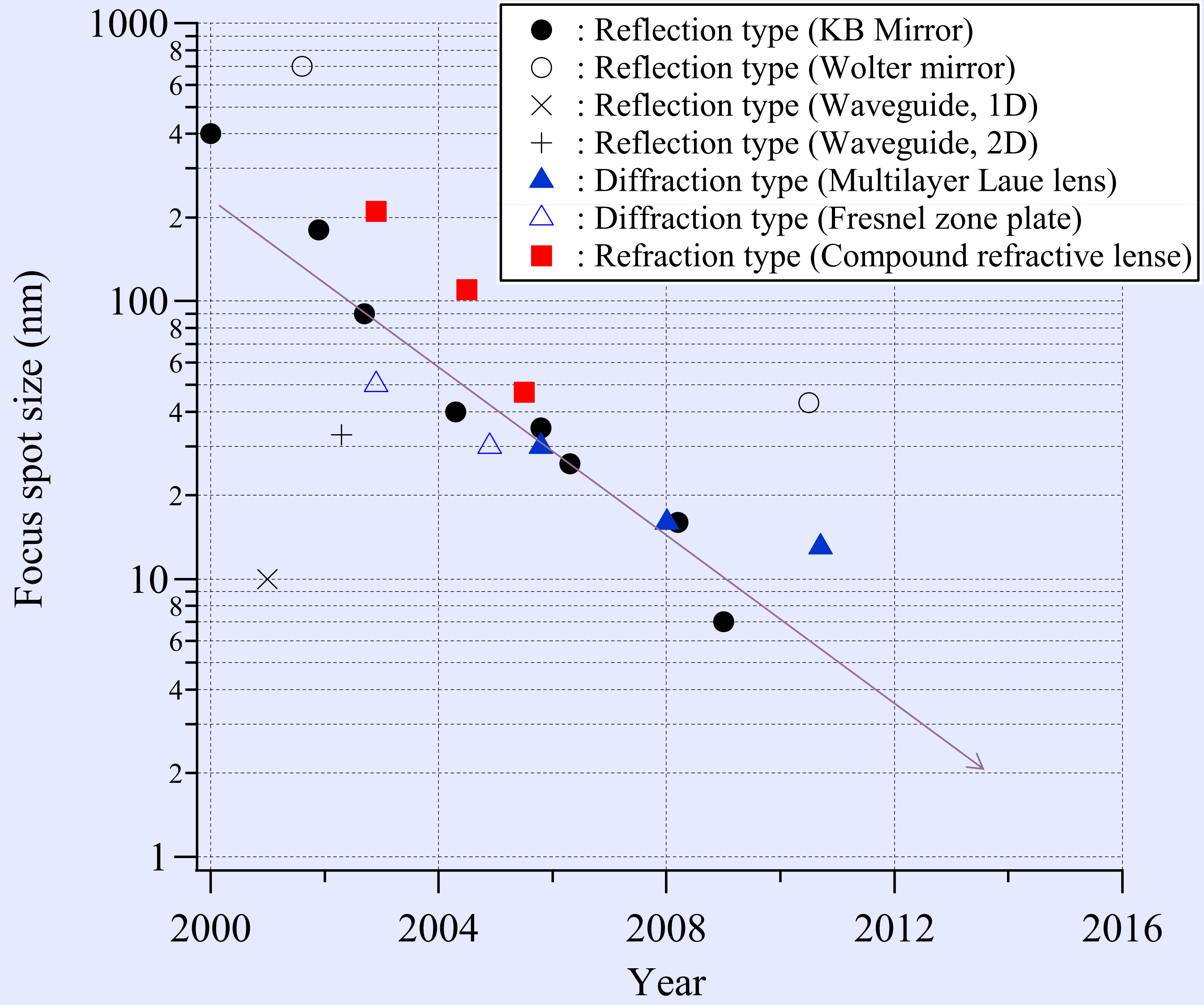

X-ray Imaging Microscopy

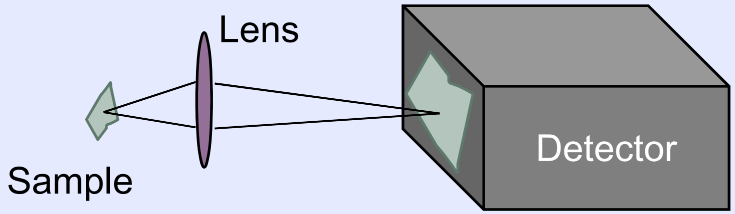

Zernike phase-contrast X-ray microscopy[1]

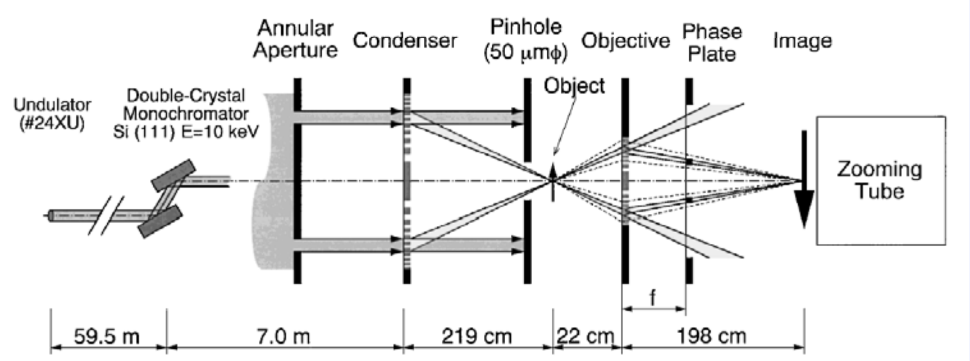

Talbot-type X-ray phase-difference microscopy[2,3]

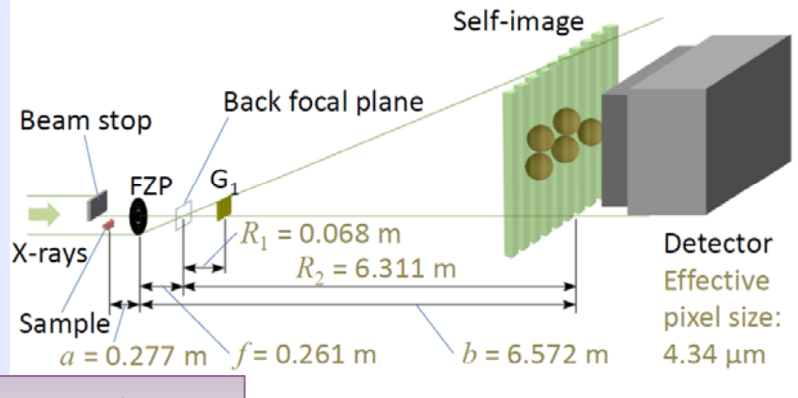

Conidium of Curvularia species

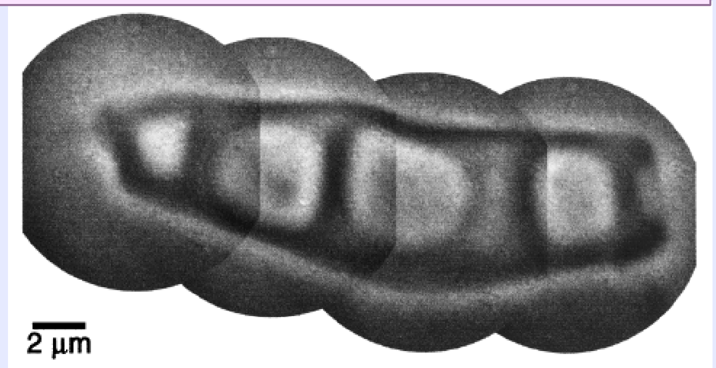

Siemens star chart

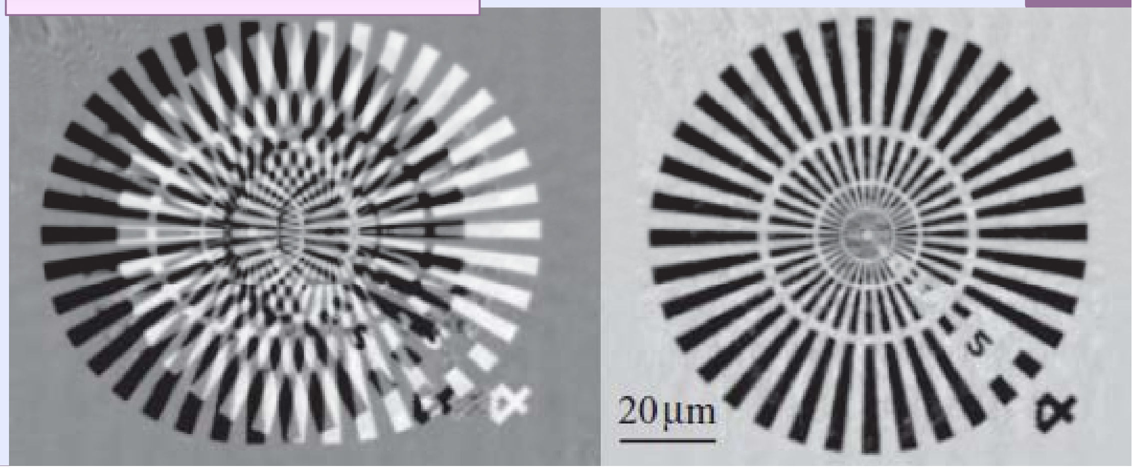

1. Y. Kagoshima *et al.*, *Jpn. J. Appl. Phys.* **40** (2001) L1190.
2. W. Yashiro *et al.*, Phys. Rev. Lett. **103** (2009) 180801.
3. W. Yashiro *et al.*, Phys. Rev. A **82** (2010) 043822.

Scanning Transmission X-ray Microscopy (STXM)

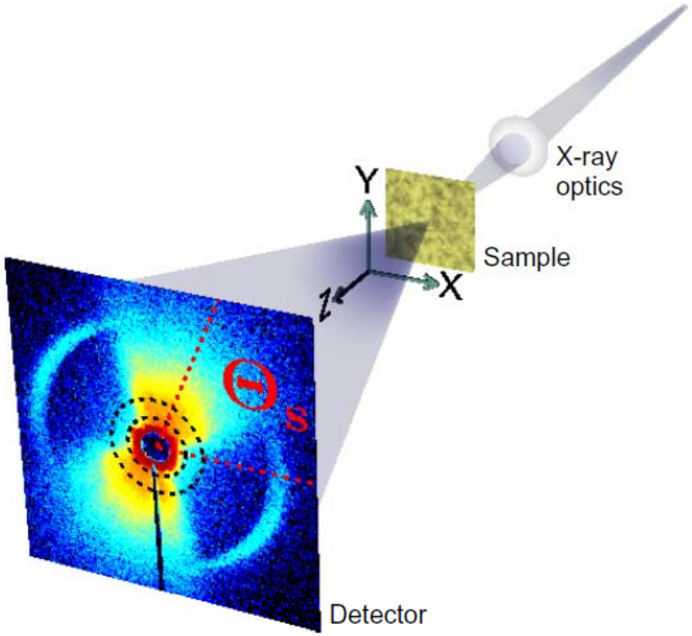

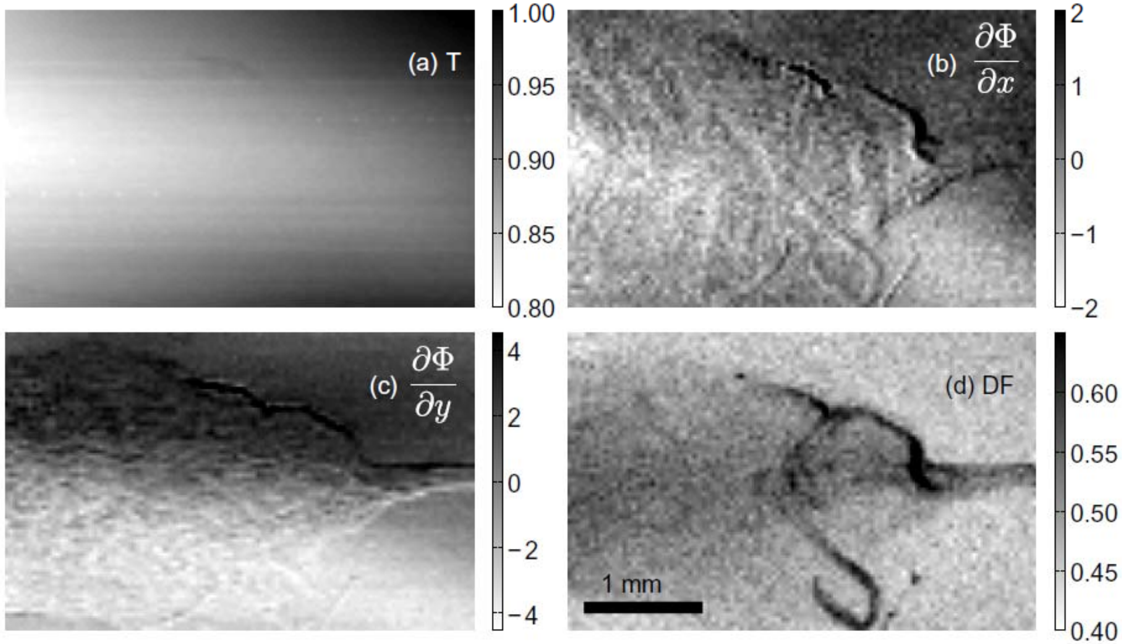

O. Bunk *et al.*, New J. Phys. 11 (2009) 123016.

Absorption image
Differential phase image
Small angle X-ray scattering image, Dark field image
Fluorescent X-ray image
…

X-ray Diffraction Microscopy

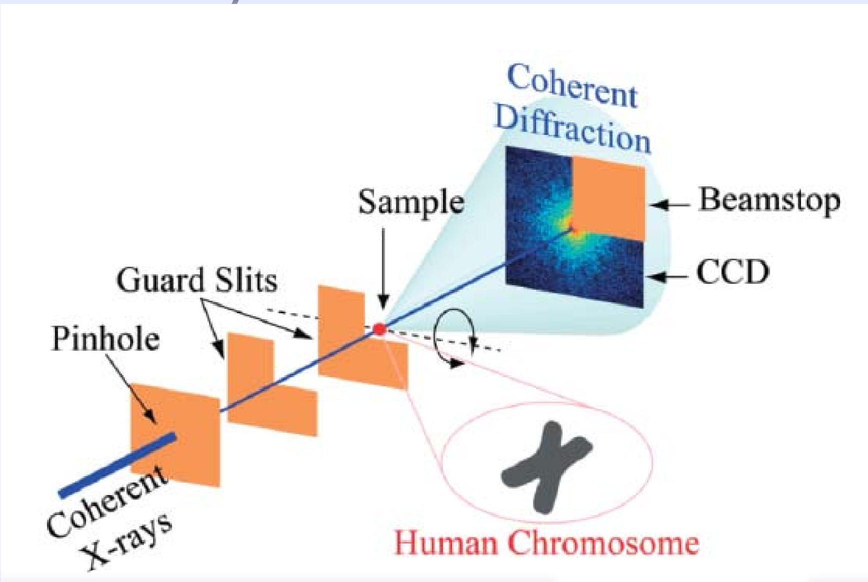

- Using coherent X-ray beam
- Measuring intensity of diffracted X-rays

A few nanometer spatial resolution imaging

Coherent diffraction pattern

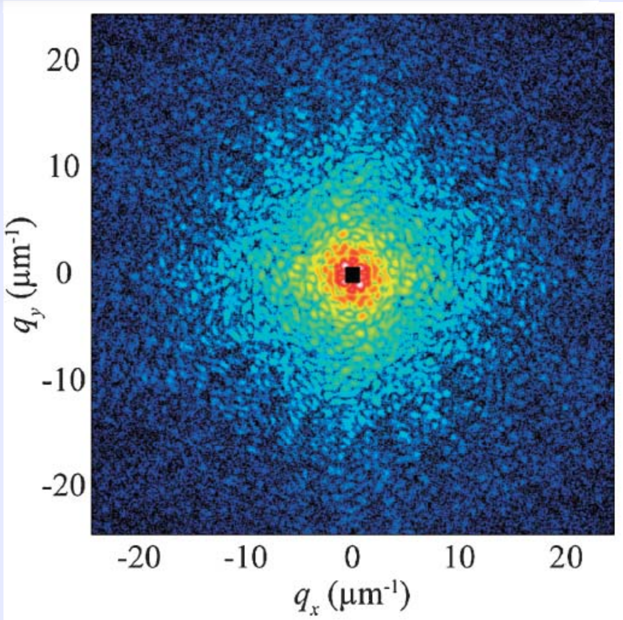

Human chromosome

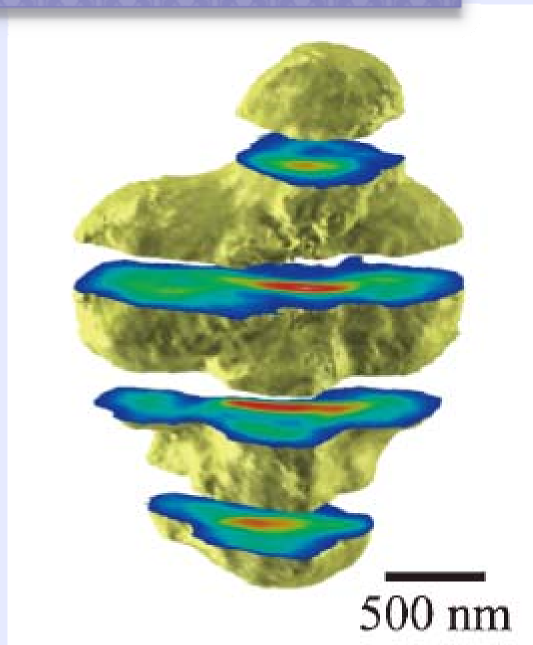

Y. Nishino *et al.*, *Phys. Rev. Lett.* **102** (2009) 018101.

Phase problem in X-ray diffraction

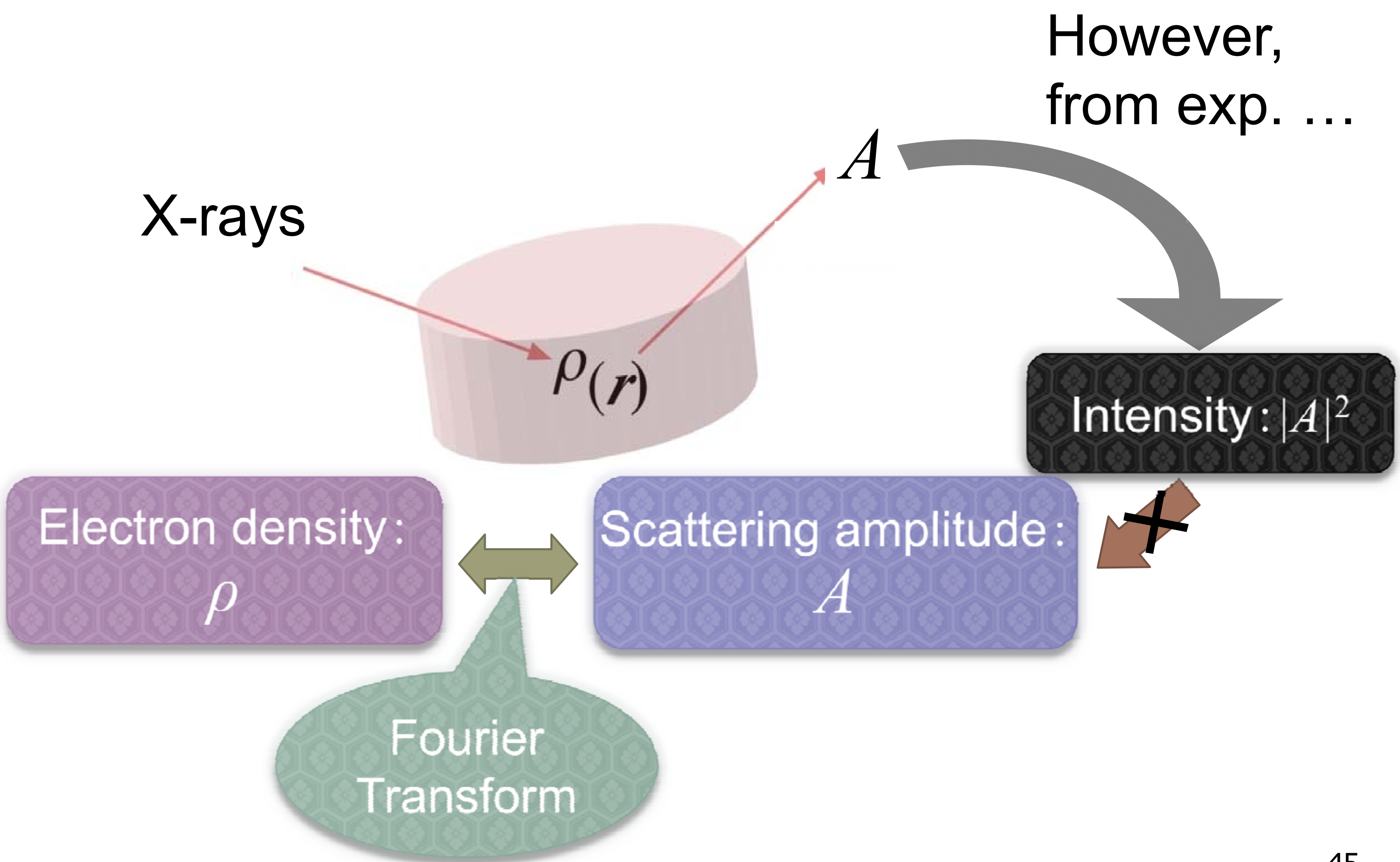

Oversampling & iterative phase retrieval algorithm

Oversampling

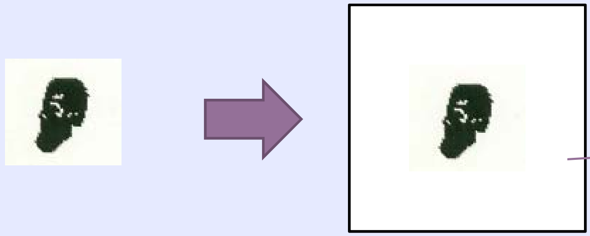

Smaller than FOV
Zero (known) density around the sample

Iterative phase retrieval algorithm

Random $\rho(\mathbf{r})$ $\rightarrow$ $\rho(\mathbf{r}) \xrightarrow{\text{FT}} G(\mathbf{K}) = |G(\mathbf{K})| e^{i\varphi(\mathbf{K})}$

$G'(\mathbf{K}) = |F(\mathbf{K})| e^{i\varphi(\mathbf{K})} \xrightarrow{\text{FT}^{-1}} \rho'(\mathbf{r})$

Real-Space Constraints

Reciprocal-Space Constraints

$$\rho_{n+1}(\mathbf{r}) = \begin{cases} \rho'_n(\mathbf{r}) & \text{(in support)} \\ 0 & \text{(outside)} \end{cases}$$

$|F(\mathbf{K})|$: intensity of diffracted X-rays obtained experimentally

Retrieval of real space image (simulation)

Diffraction intensity ($|A|^2$, no phase information)

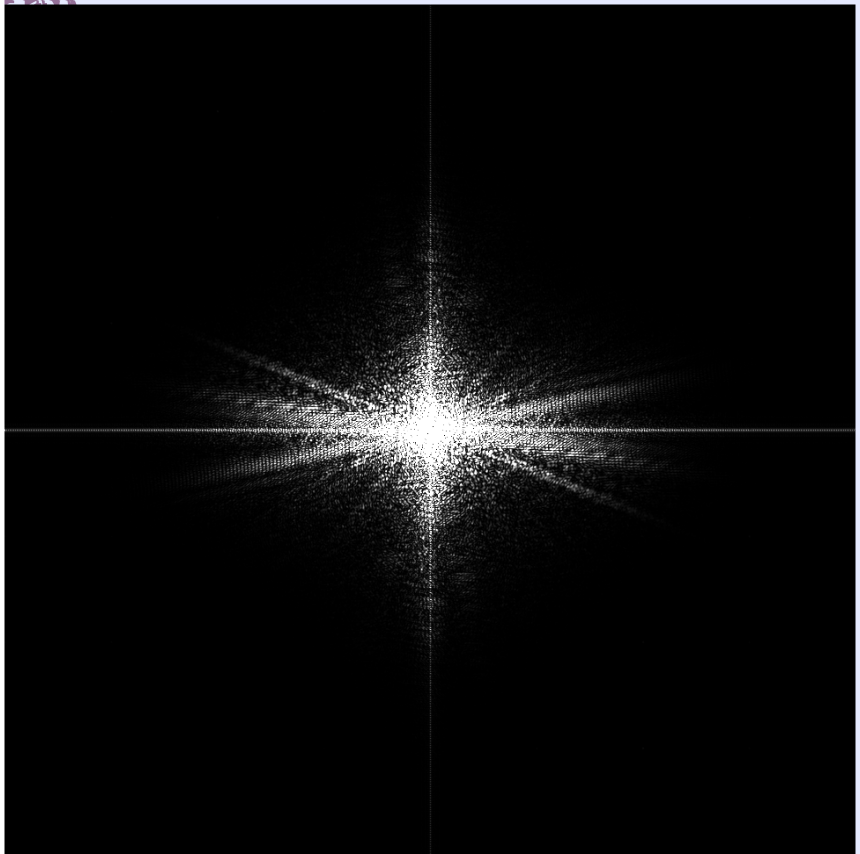

Retrieved real space image

Summary

- X-ray transmission imaging
  - Conventional X-ray absorption imaging/tomography
  - X-ray phase imaging/tomography
    - Complex refractive index
    - Advantage of using X-ray phase information
    - Three examples of X-ray phase imaging techniques
      - Interference
      - Fresnel diffraction
      - Refraction

Spatial coherence

  - X-ray microscopy
    - Optics for X-ray microscopy
    - Three examples of X-ray microscopies
      - Imaging microscopy
      - Scanning microscopy
      - Diffraction microscopy

Types of X-ray imaging

Transmission

Geometric optics

radiography, tomography, topography, lithography, laminography, tomosynthesis, etc.

Wave optics

imaging microscopy, holography, fluorescent holography, phase imaging/tomography, lithography, etc.

Scanning probe

scanning microscopy, fluorescent tomography, phase imaging, etc.

Diffraction

coherent diffraction imaging, ptychography.

Refractive index in the X-ray region

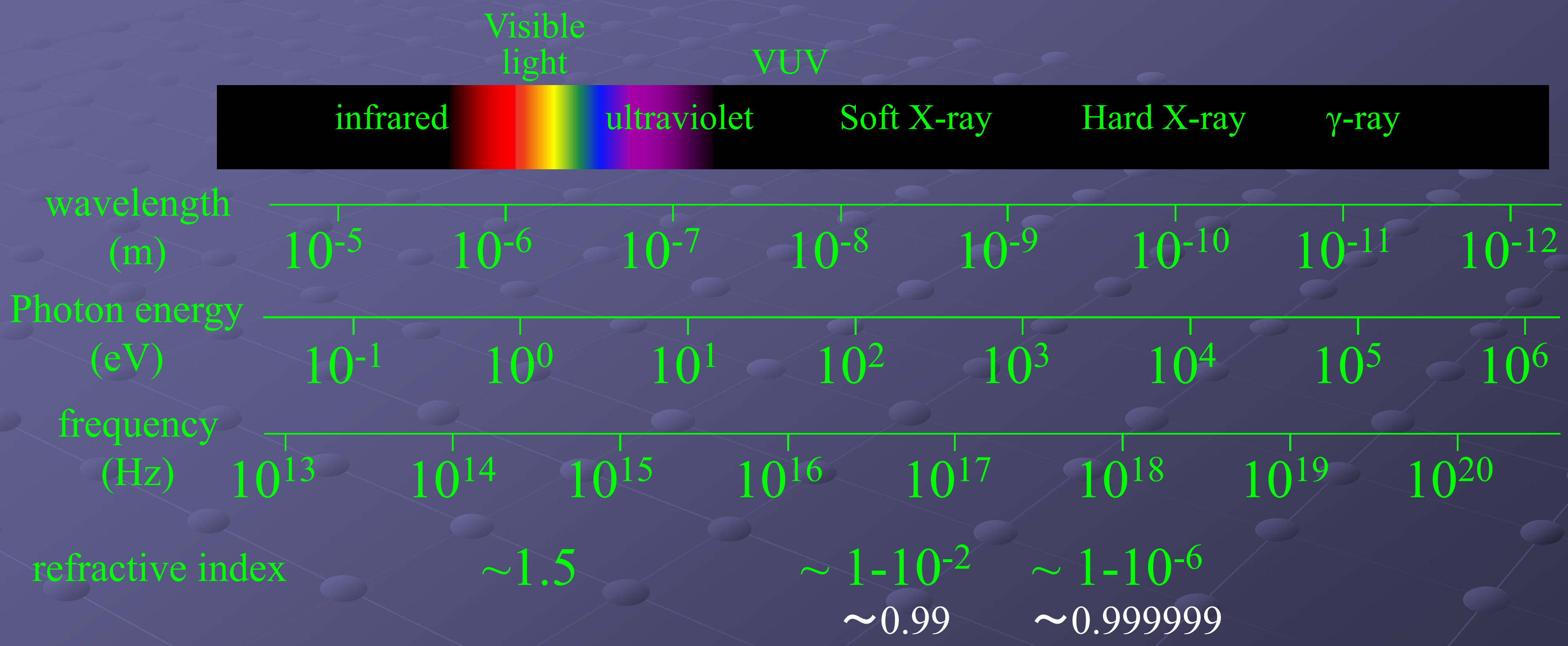

Using X-ray interference

Same phase

Opposite phase

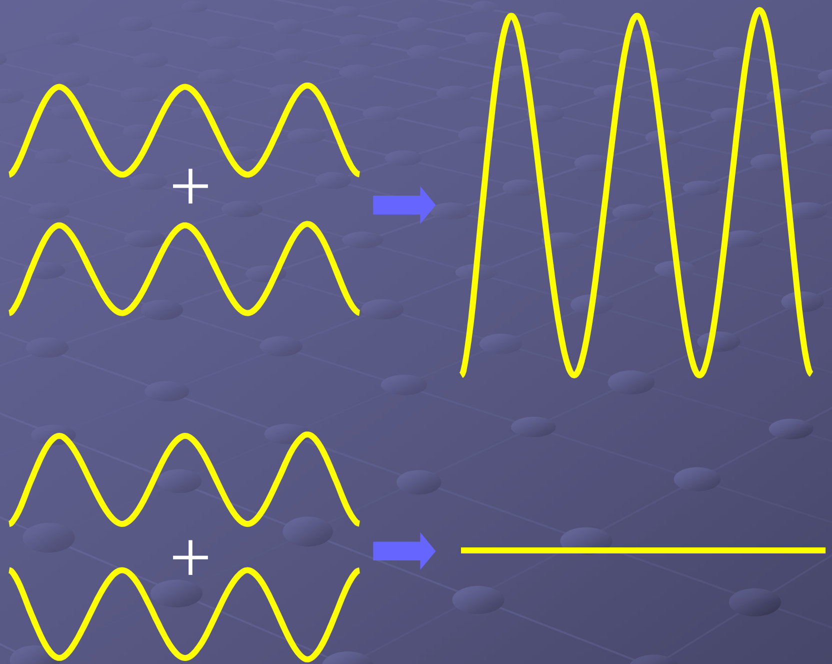

Mechanical stability should be much smaller than X-ray wavelength ($<10^{-11}$ m).

Two-beam interferometry

A. Momose & J. Fukuda, *Med. Phys.* 22 (1995) 375

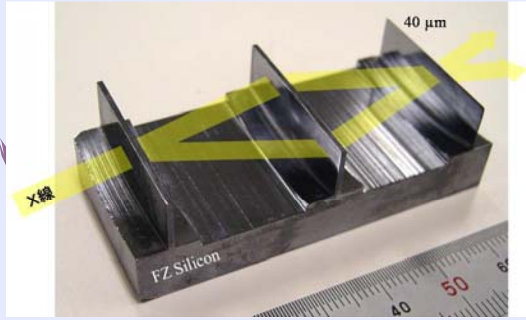

X-ray interferometer

Interference image 1 mm

Transmission image 1 mm

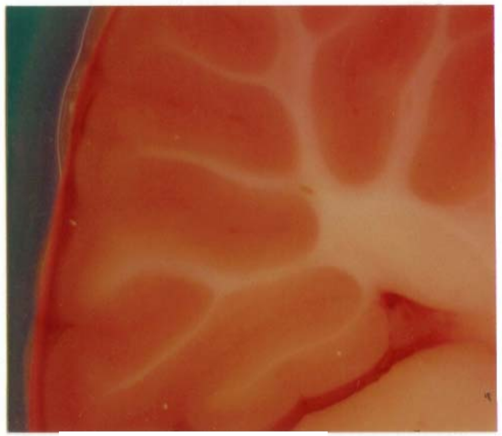

Optical image 1 mm

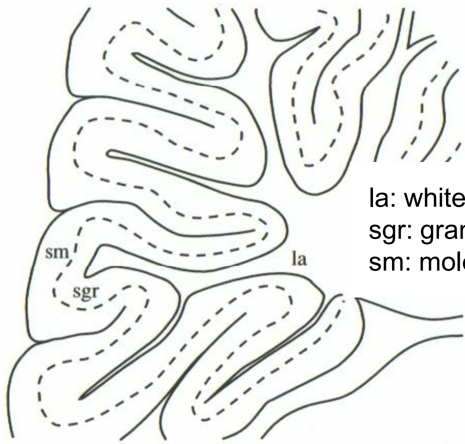

la: white matter
sgr: granular stratum
sm: molecular layer

Rat cerebellum (1mm thick)
@ 12.4 keV (PF)

Two-beam interferometry

Blood vessels in mouse liver; blood was replaced with saline.

E = 17.7 keV

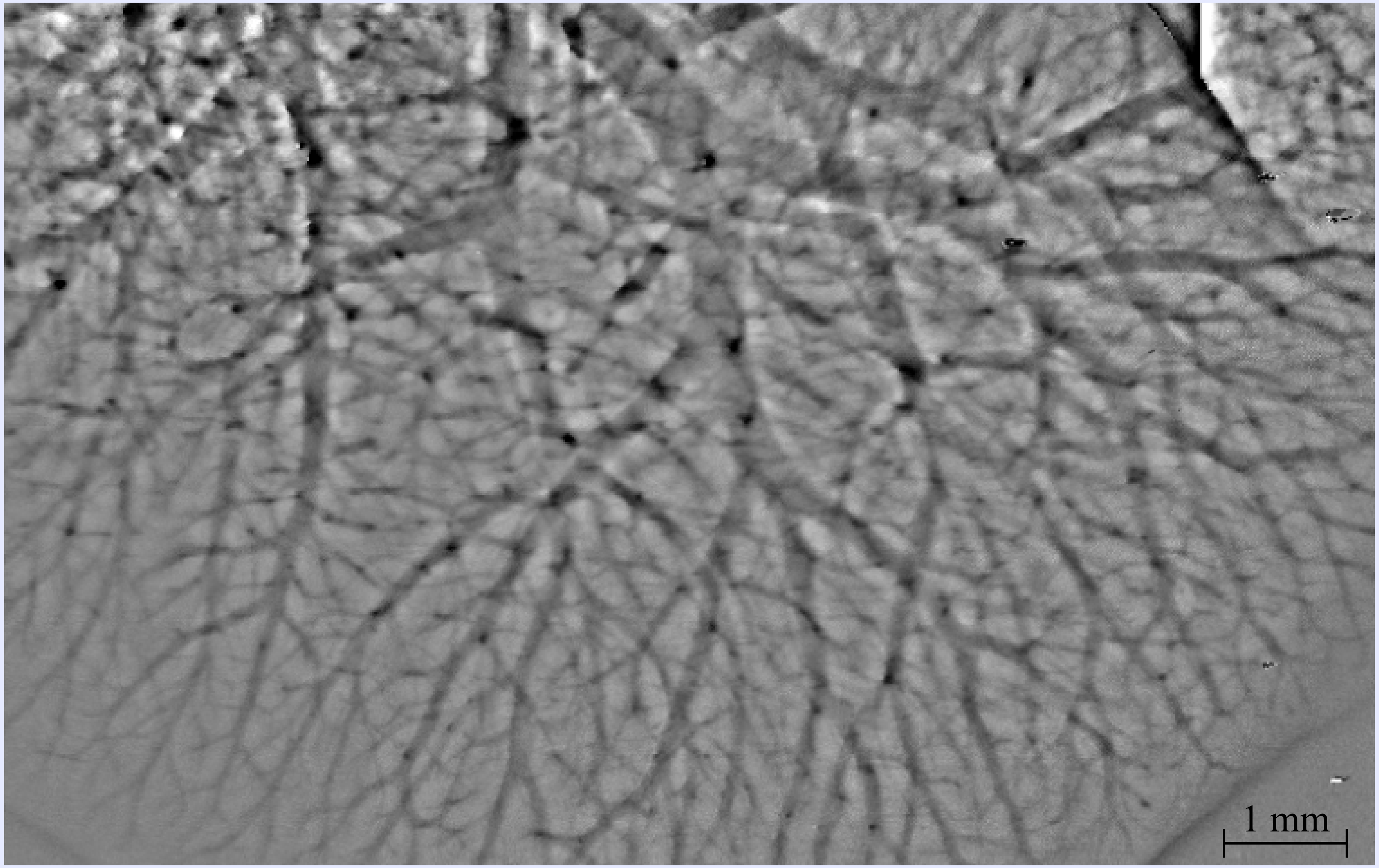

A. Momose et al.：Oyo Butsuri 71（2002）1148

Phase tomogram

@12.4 keV

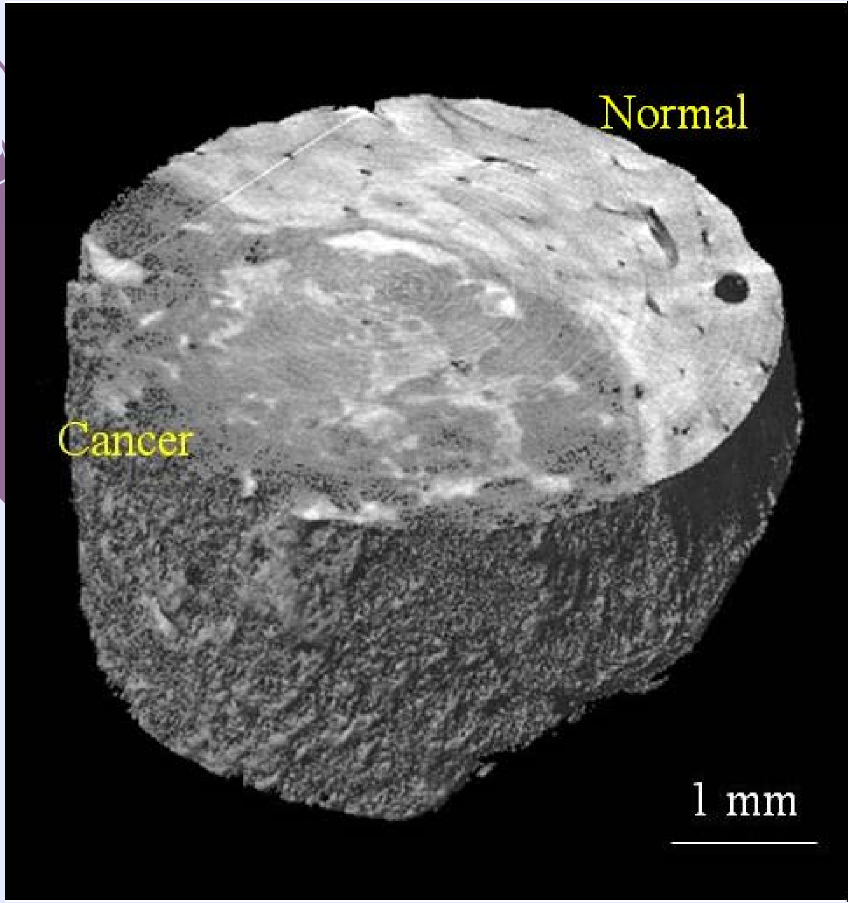

rabbit liver

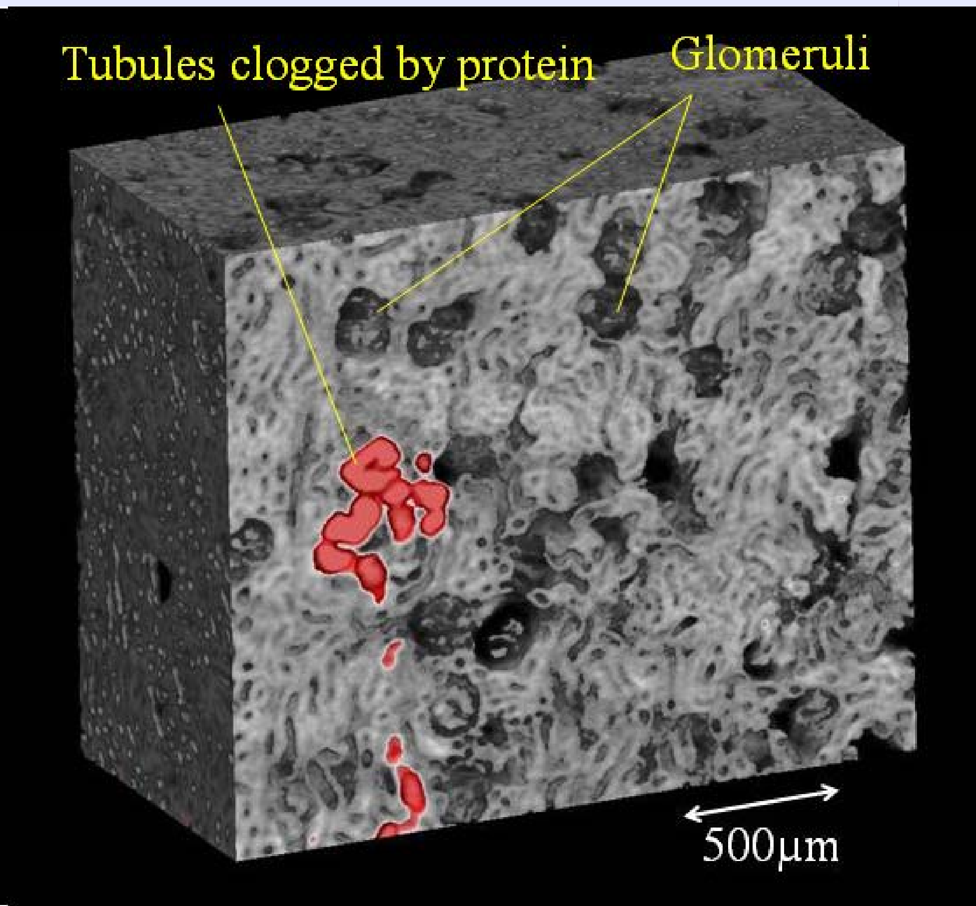

rat kidney

Analyzer-based method with transmission gratings

Talbot Interferometry

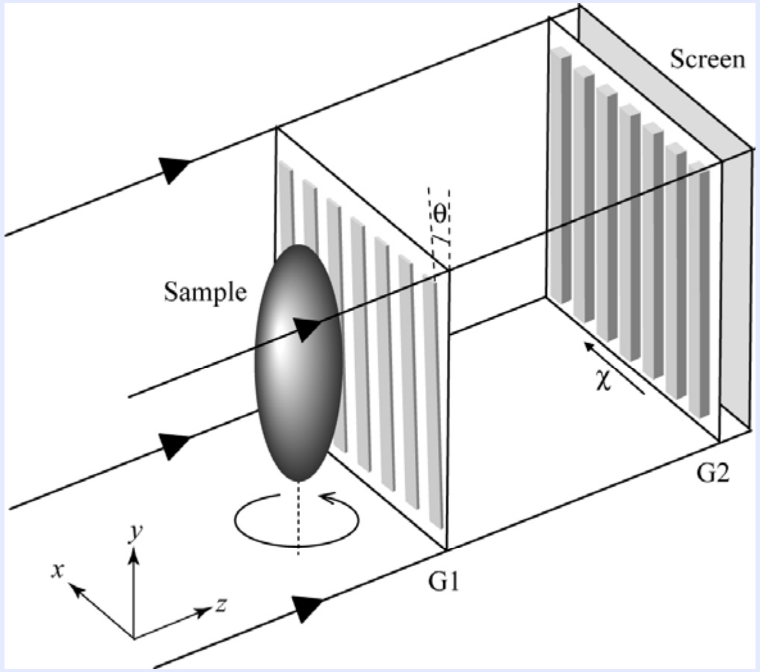

Advantages of the X-ray Talbot interferometry

- Experimental arrangement is very simple.
- High mechanical stability is not necessary.
- A wide area imaging is possible.
- Polychromatic X-rays is available (it functions with a much broader energy band width than in the case of using crystal interferometry).
- Divergent X-rays is also available.

The X-ray Taltot interferometry functions with **a compact laboratory X-ray source.**

Application to medical diagnostics

Next Step —X-ray Talbot-Lau Interferometer—

Talbot interferometer coherence length > grating pitch

↳ Microfocus X-ray generator Low power Long exposure

Talbot-Lau interferometer functions with any X-ray sources

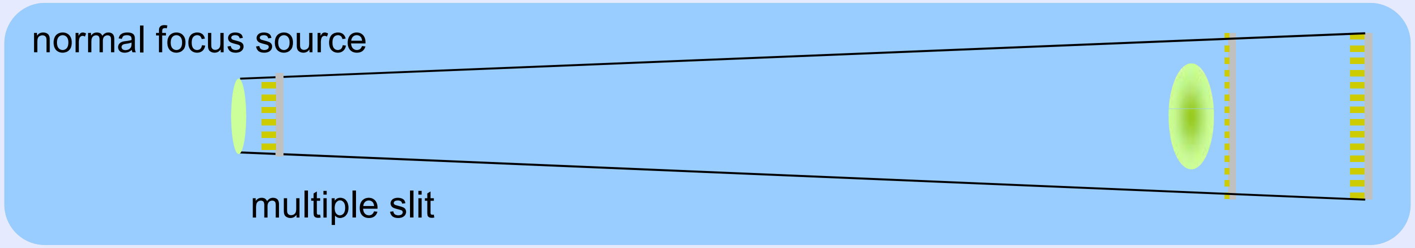

The spacing of a multiple-slit is determined so that fringes generated by X-rays from each slit are overlaid constructively.

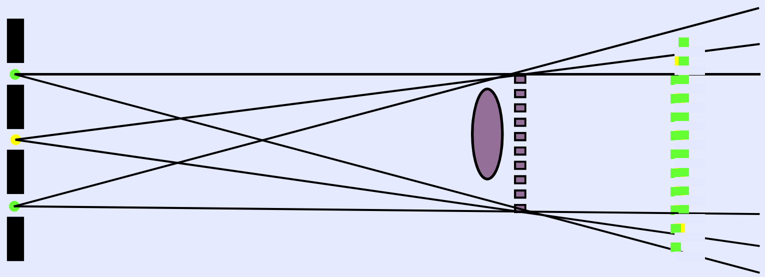

F. Pfeiffer et al., *Nat. Phys.* **2** (2006) 258.

Talbot-type X-ray microscope @ SP8

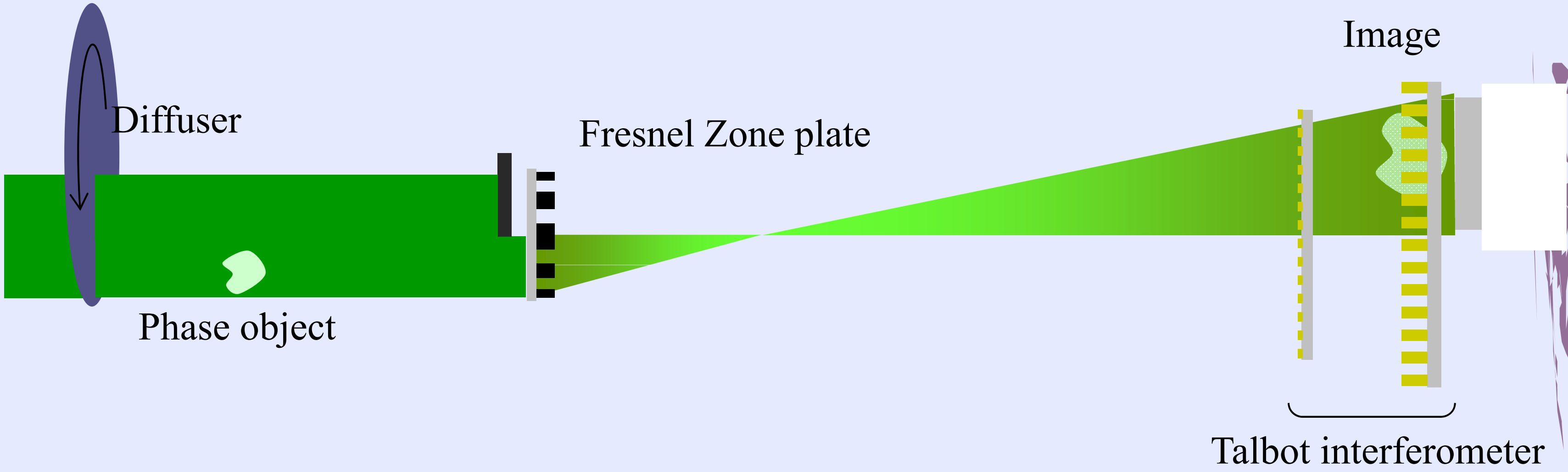

@ 12.4 keV

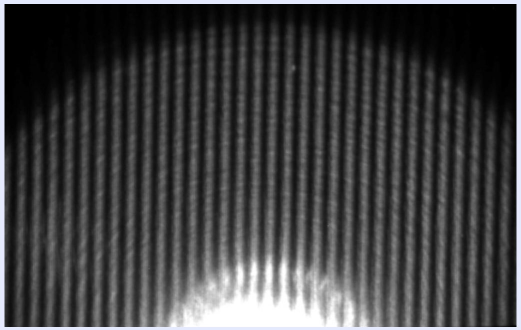

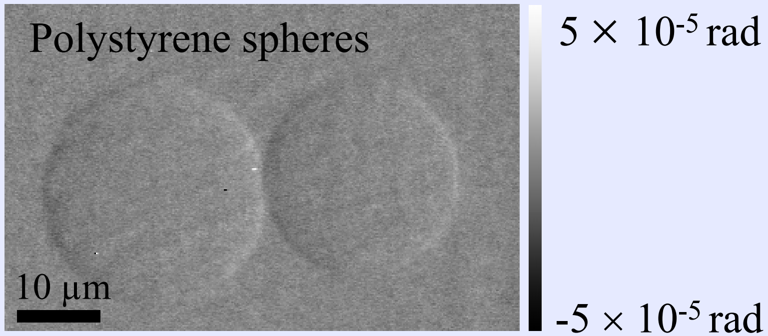

A. Momose et al., SPIE Proc. 6318 (2006)

Recent progress of the X-ray Talbot interferometry

Talbot-Lau interferomtry

Short time measurement by a normal-focus compact laboratory source

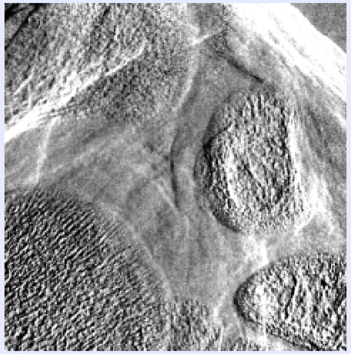

Differential phase image of cartilage of a chicken wing

Visibility contrast imaging

The ‘third’ image

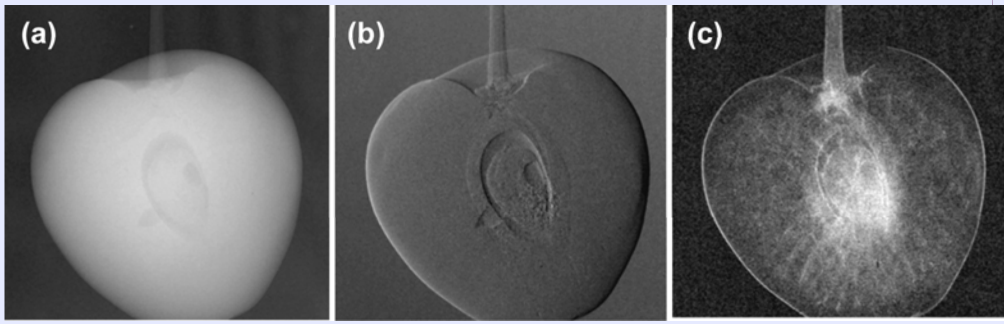

Absorption contrast image of a cherry

Differential phase image

Visibility contrast image

High-speed X-ray phase imaging (4DCT)

High-speed image using white synchrotron radiation beam

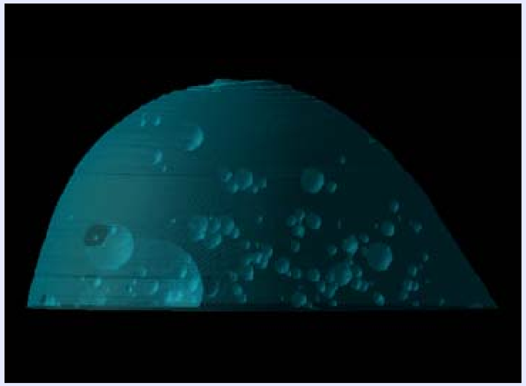

In situ observation of glue
(A. Momose and W. Yashiro *et al. Opt. Exp.* (2009), **17** (2009) 12540).

Phase-difference X-ray imaging microscopy

High spatial resolution and high sensitivity

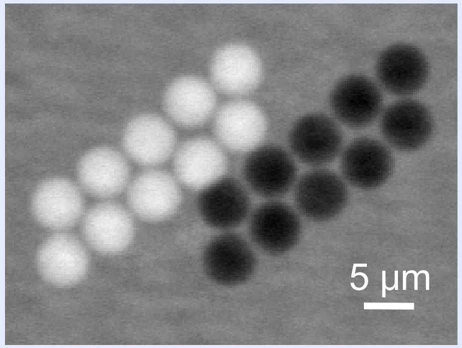

Phase-difference image of polymer spheres
(W. Yashiro *et al. Phys. Rev. Lett.* **103** (2009), 180801).

From Talbot Effect To X-ray Phase Imaging

1836 Talbot Effect (W. H. F. Talbot)

1971 Talbot Interferometry
(S. Yokozeki and T. Suzuki)
(A. W. Lohmann and D. E. Silva)

1988 Soft X-ray Talbot Effect (V. V. Aristov *et al.*)

1992 Talbot-Lau Interferometry (J. F. Clauser *et al.*)

1997 Hard X-ray Talbot Effect (P. Cloetens *et al.*)

2003 Hard X-ray Talbot Interferometry (A. Momose *et al.*)

2006 Hard X-ray Talbot-Lau Interferometry (F. Pfeiffer *et al.*)

Amplitude attenuation vs. phase shift

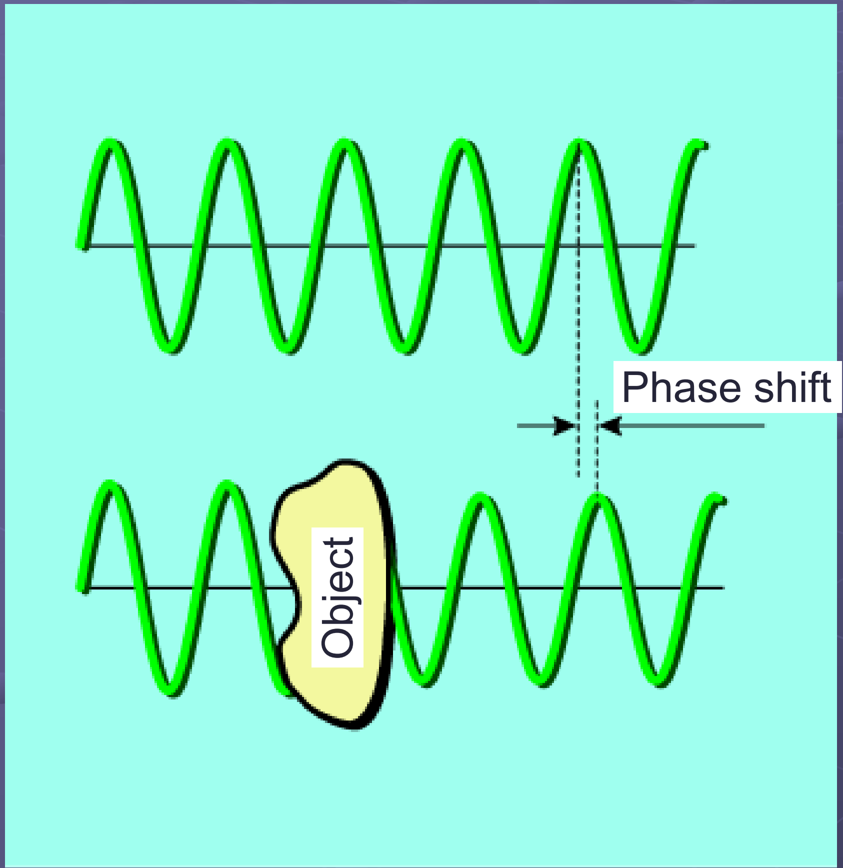

- Amplitude of the wave decreases by absorption by the object.
- Phase of the wave shifts by the difference in velocity of the wave in the object

$$v_{obj} = v_o / n$$

$$n : \text{refractive index}$$

Amplitude attenuation
→ absorption contrast imaging

Phase shift
→ phase contrast imaging

Phase shift and Refraction

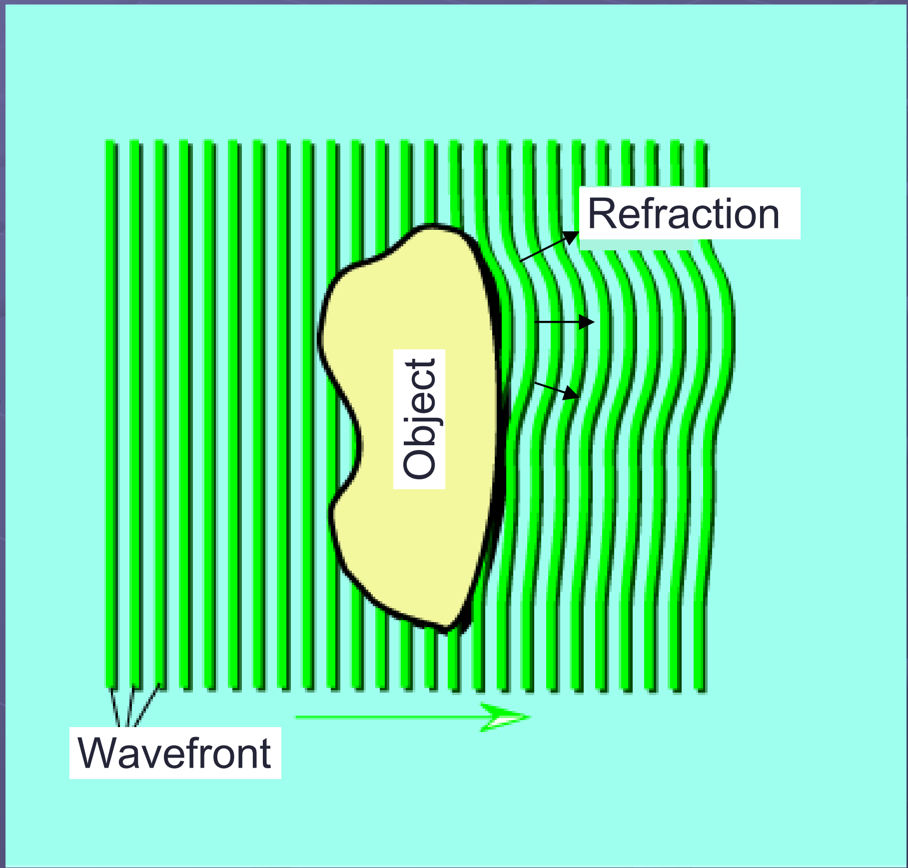

Spatially variant phase shift bends wavefront.

Wave propagates locally in the direction perpendicular to wavefront; that is, wave is refracted.

Phase shift and refraction are essentially the same phenomenon.

Phase Tomography

Rabbit liver with cancer (VX2)

@ SPring-8, BL20XU
@12.4 keV

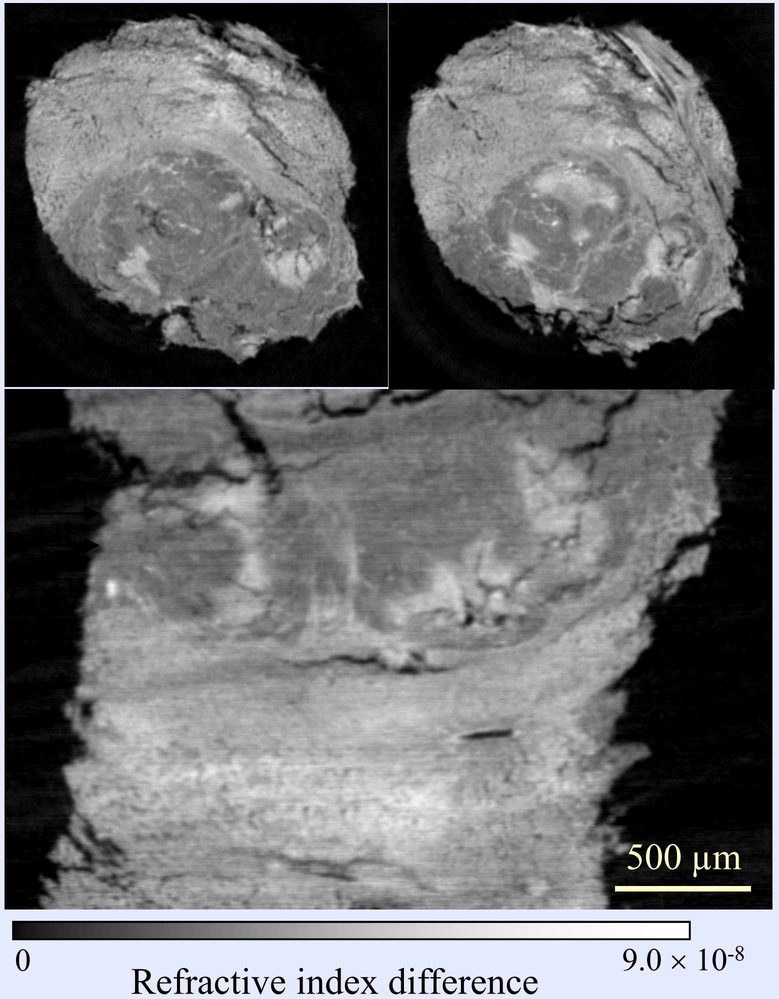

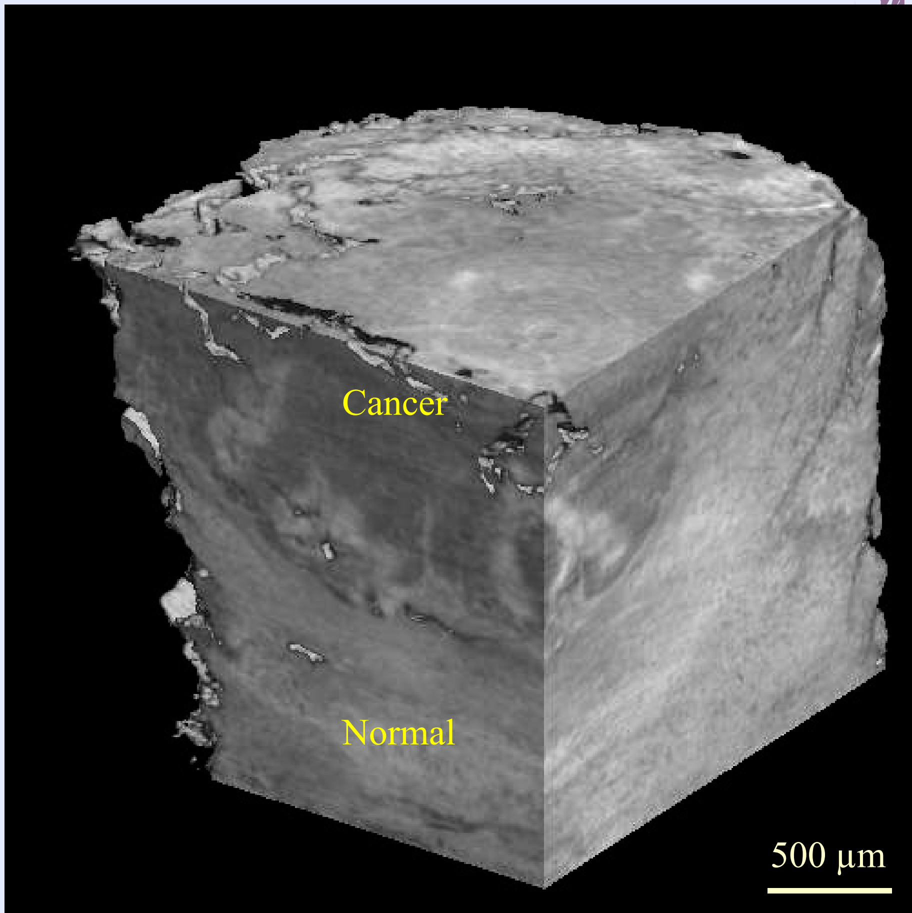

Phase Tomography
Mouse Tail

@17.7 keV

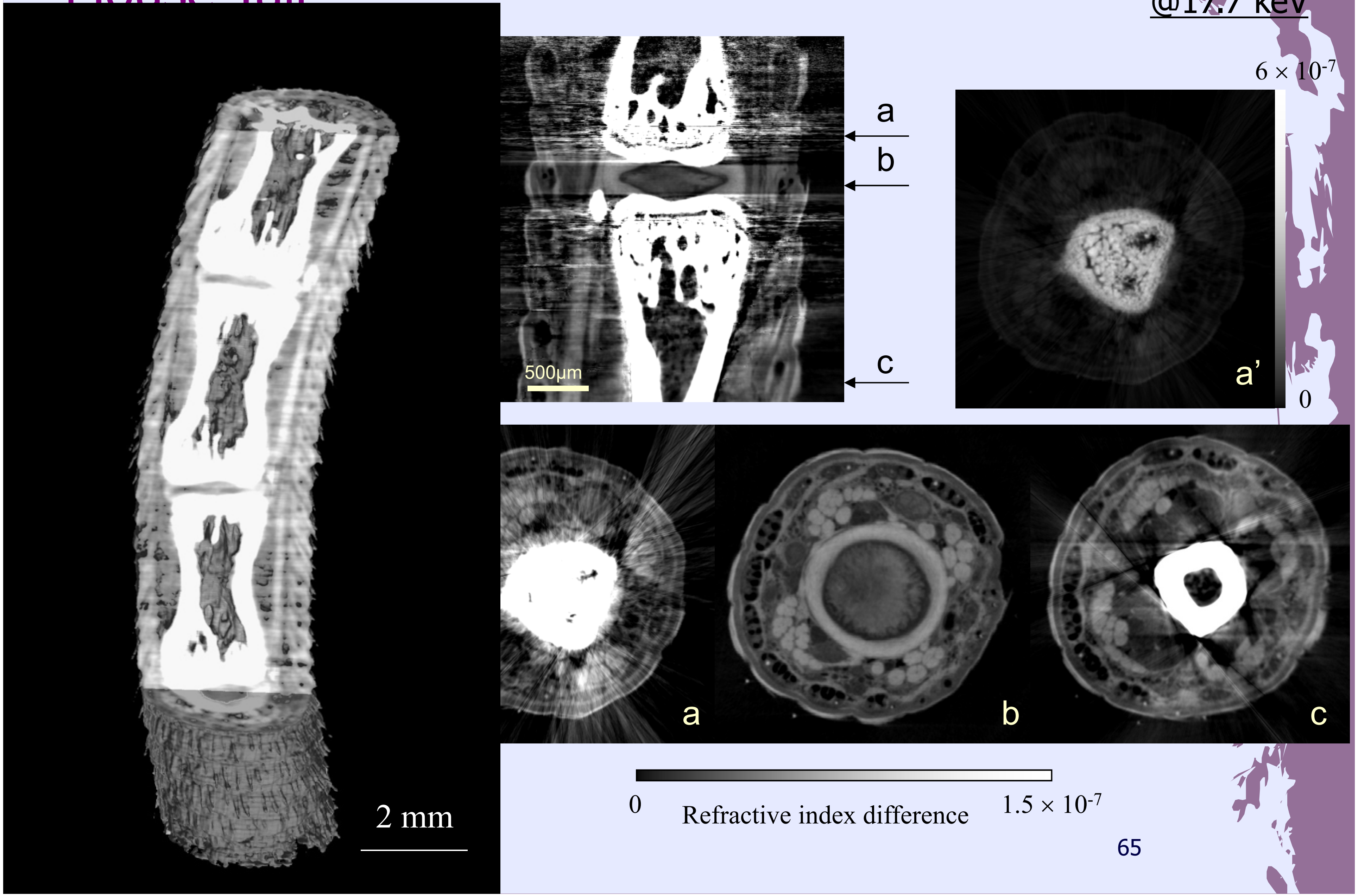

Propagation-based method

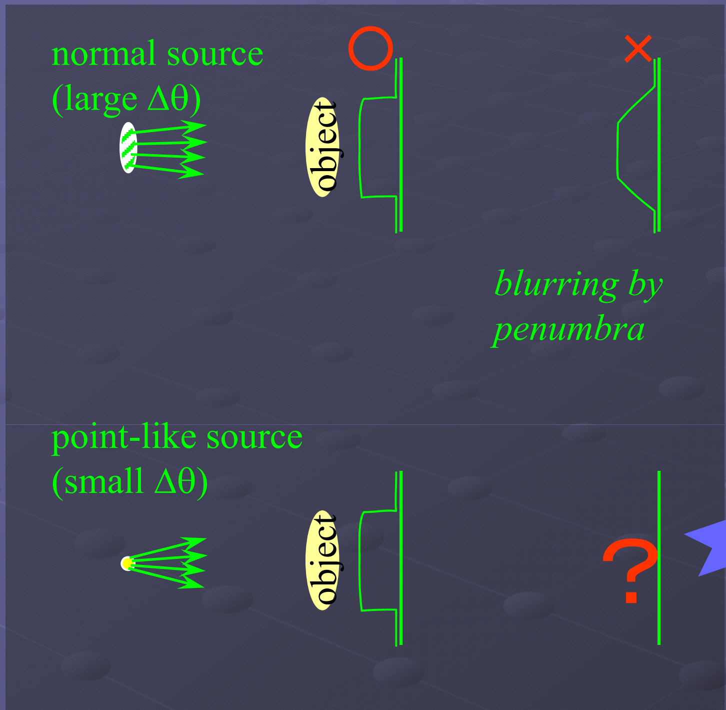

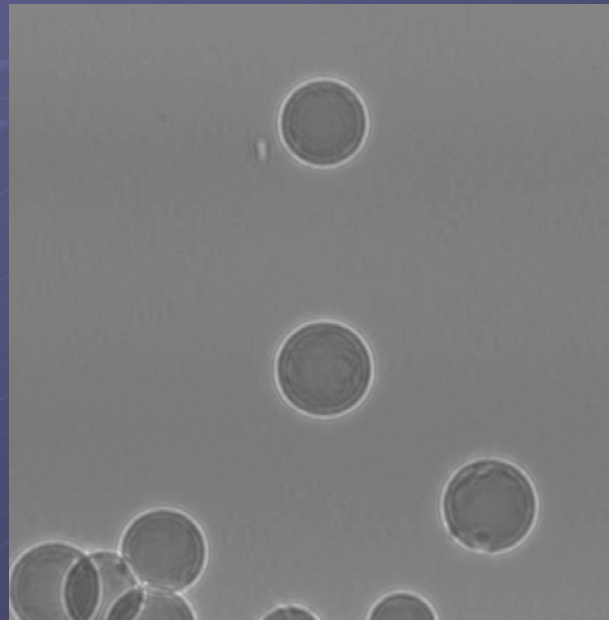

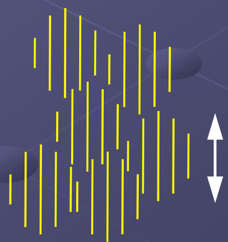

$$\frac{\lambda}{\Delta\theta}$$ (spatial coherence length)

Δθ: angular diameter of source at the object

4D tomography

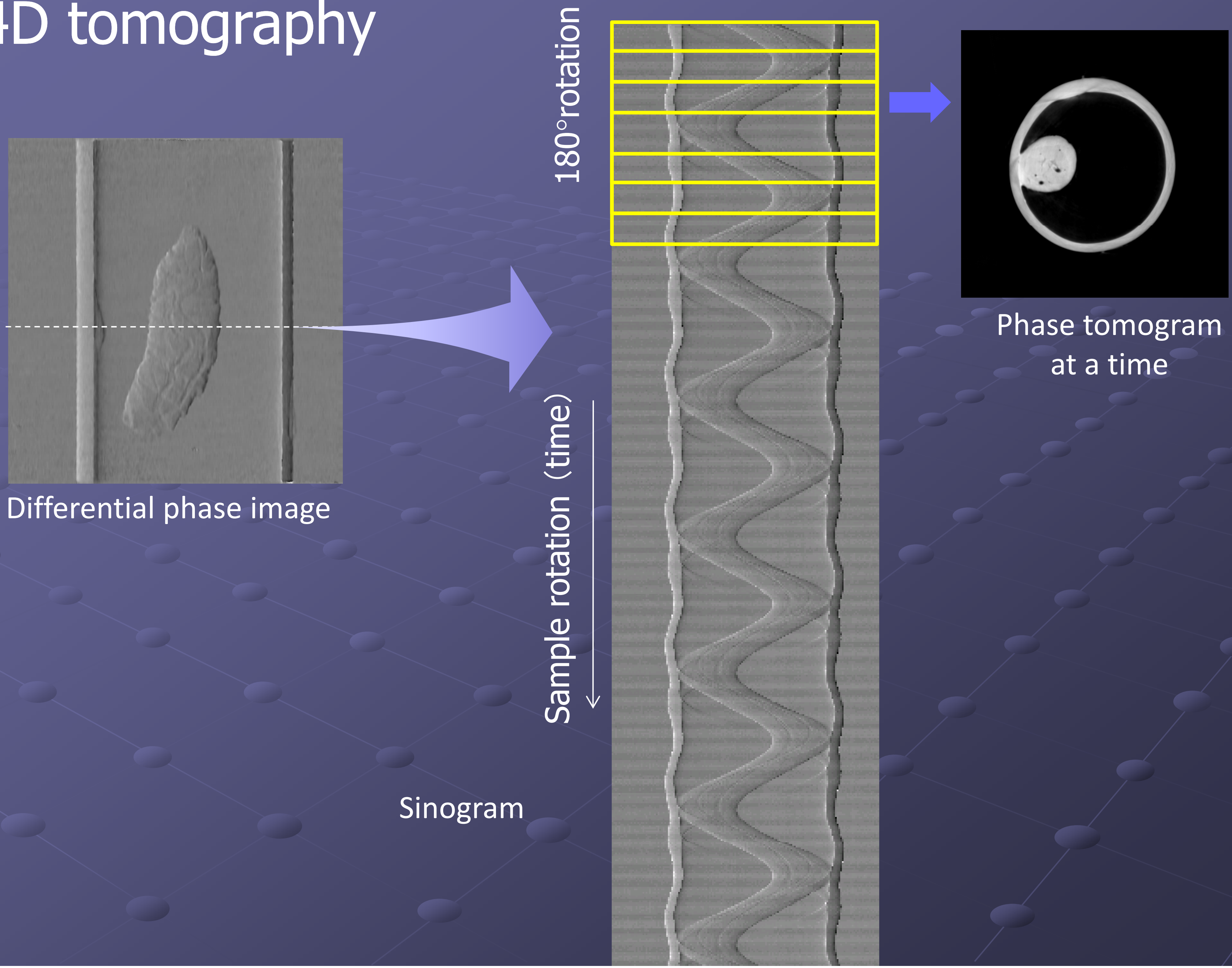

Oversampling & iterative phase retrieval algorithm —An example

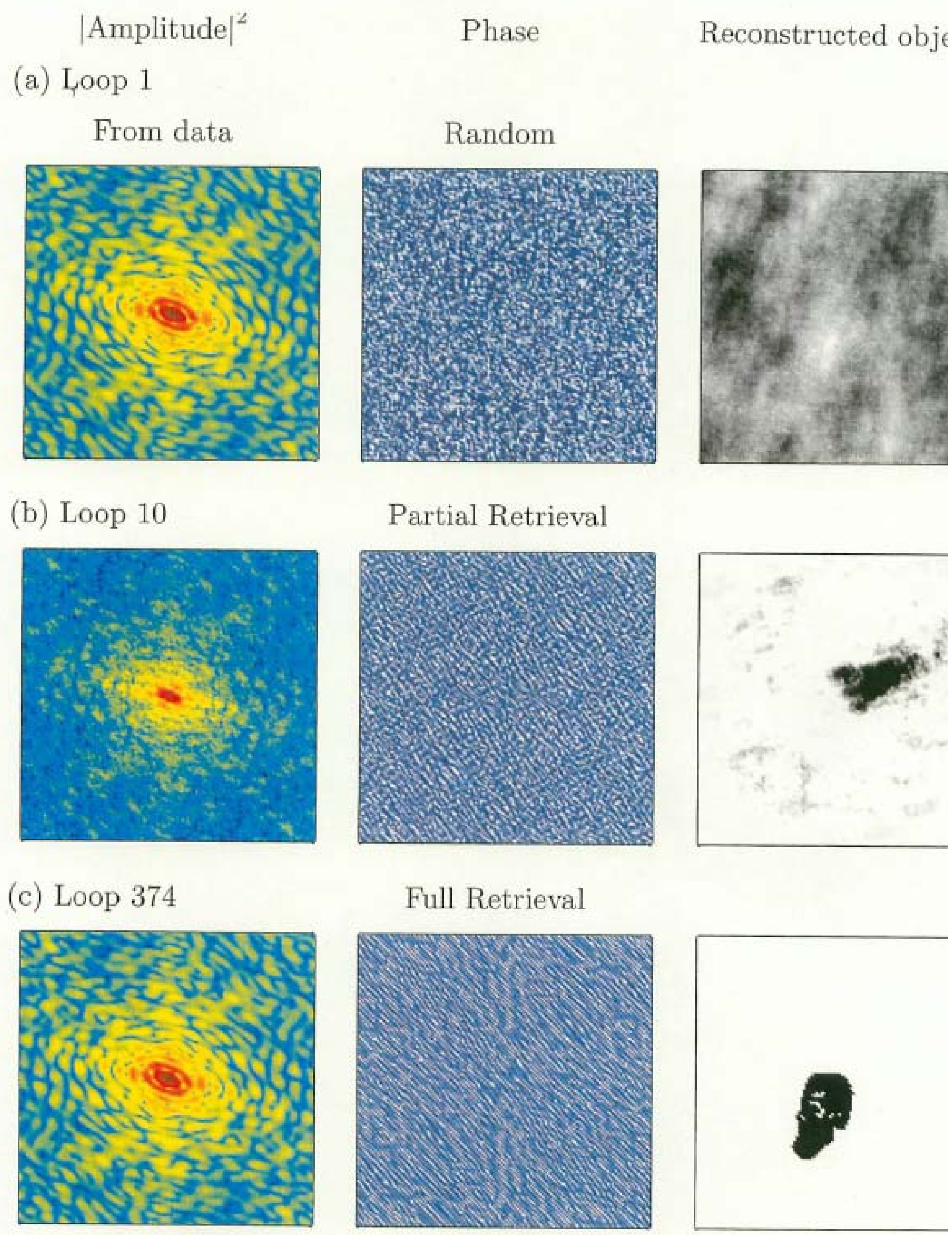

J. Als-Nielsen & D. McMorrow, "Elements of Modern X-ray Physics", 2nd ed. (2011).

confidential

Retrieval of differential phase image —Fourier transform method—

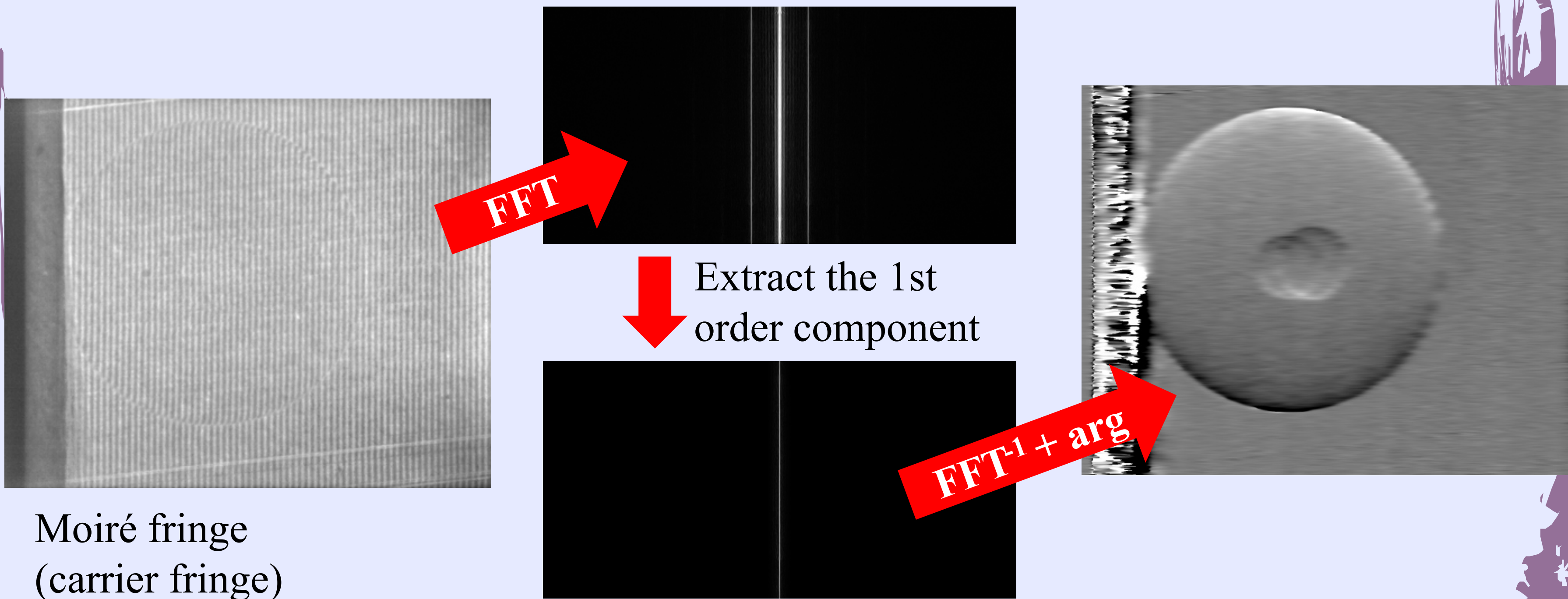

- Differential phase image can be obtained by a moiré image.
- Spatial resolution in the direction perpendicular to the moiré fringe is determined by the period of the fringe.

A. Momose, W. Yashiro, H. Maitake, and Y. Takeda, Opt. Express 17 (2009) 12540

Principle of Tomography

Fourier slice theorem

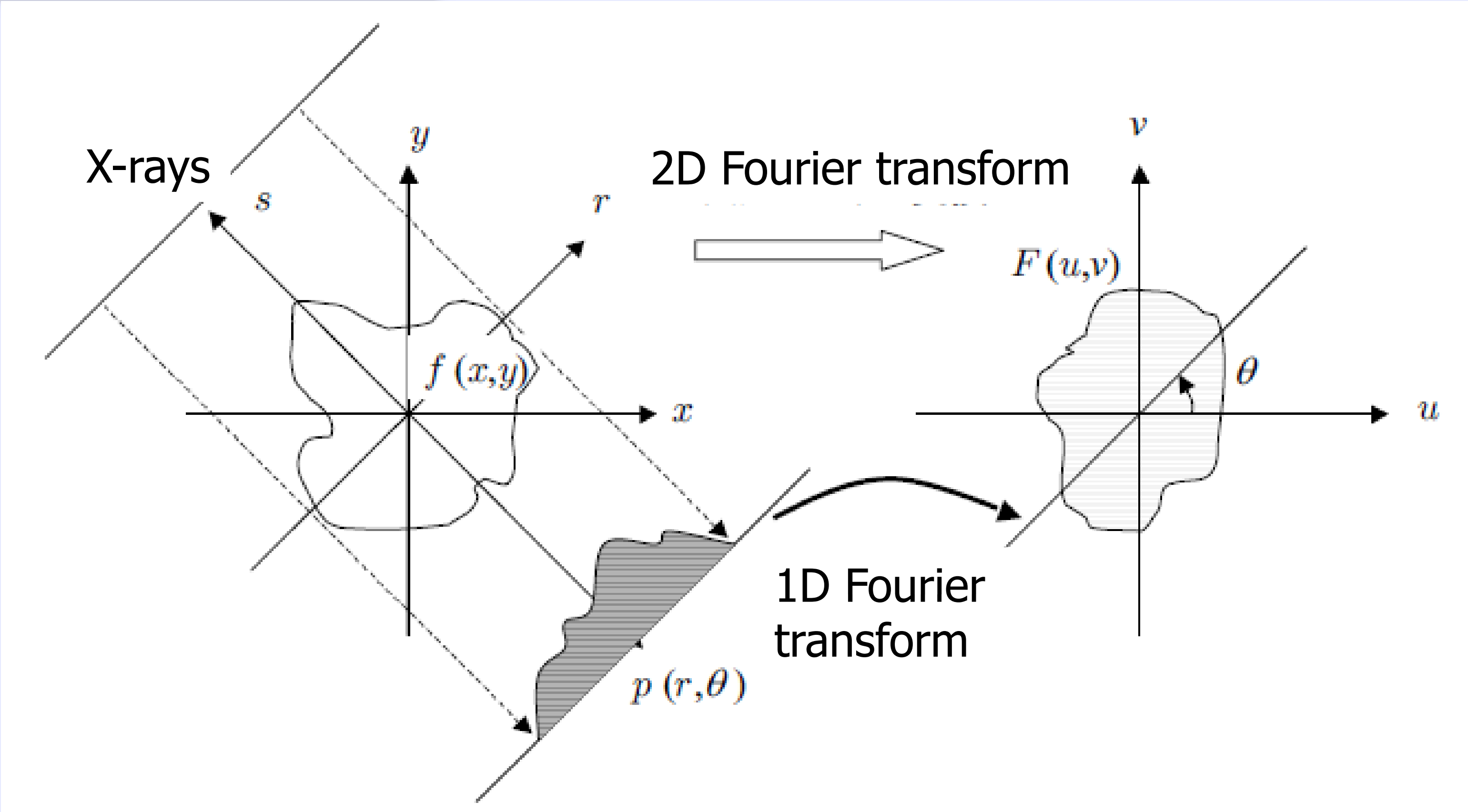

Projections $p(r,\theta) = \int f(x,y)ds$

at different projection angles (θs) ⇒ $f(x,y)$

Origin of Contrast of X-ray Absorption Imaging

Beer-Lambert Law

$$\frac{dI}{dz} = -\mu I$$

I : intensity of X-rays

μ : absorption coefficient

Attenuation of X-rays by a uniform material

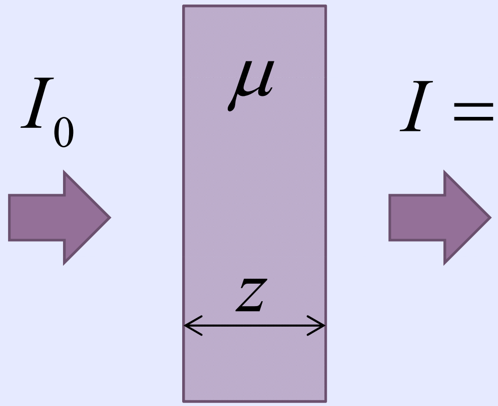

$$I = I_0 \exp(-\mu z)$$

Intensity of transmission X-rays

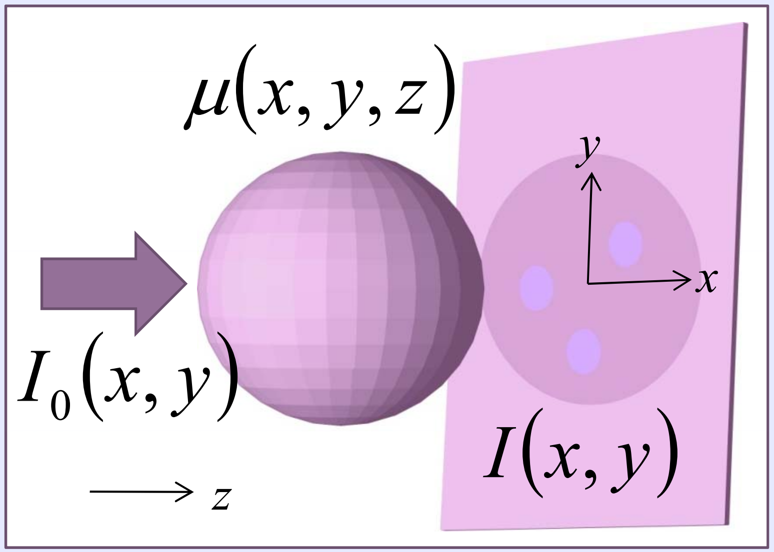

Projection of μ

$$I = I_0 \exp\left(-\int \mu(x, y, z)\,dz\right)$$

$$\boxed{\int \mu(x, y, z)\,dz = -\log\left(\frac{I}{I_0}\right)}$$

Examples of complex refractive index

Complex refractive indices at 20 keV

material	δ	β	δ/β
poly-styrene	5.0×10^{-7}	3.2×10^{-10}	1.6×10^{3}
water	5.8×10^{-7}	6.0×10^{-10}	9.7×10^{2}
SiO_2	1.3×10^{-6}	2.9×10^{-9}	4.5×10^{2}
Si	1.2×10^{-6}	4.9×10^{-9}	2.4×10^{2}
Fe	3.8×10^{-6}	9.7×10^{-8}	3.9×10^{1}